International
Progress Report

IPR-01-71

Äspö Hard Rock Laboratory

A Discrete Fracture Network Model of the Äspö TBM Tunnel Rock Mass

Sven Follin
Jan Hermansson

Golder Associates AB

December 1996

Svensk Kärnbränslehantering AB
Swedish Nuclear Fuel
and Waste Management Co
Box 5864
SE-102 40 Stockholm Sweden
Tel +46 8 459 84 00
Fax +46 8 661 57 19

Äspö Hard Rock Laboratory

Report no.	No.
IPR-01-71	F50K
Author	Date
Follin, Hermansson	96-12-01
Checked by	Date
Approved	Date
Christer Svemar	02-03-21

Äspö Hard Rock Laboratory

A Discrete Fracture Network Model of the Äspö TBM Tunnel Rock Mass

Sven Follin
Jan Hermansson

Golder Associates AB

December 1996

Keywords: Discrete Fracture Network Modelling, Äspö HRL, TBM

This report concerns a study which was conducted for SKB. The conclusions and viewpoints presented in the report are those of the author(s) and do not necessarily coincide with those of the client.

ABSTRACT

The Äspö Hard Rock Laboratory provides excellent opportunities for measurements on fracture traces that can be used as input to numerical models. This project aims at producing a 3-D discrete fracture network (DFN) model of the rock mass proximal to the TBM tunnel in the HRL. The DFN model will serve as a platform for discussions regarding rock mechanics and ground water flow adjacent to deposition drifts and canister holes.

Keywords: Discrete Fracture Network Modeling, Äspö HRL, TBM

SAMMANFATTNING

Äspölaboratoriet ger unika möjligheter att utföra sprickmätningar som kan användas som indata till numeriska modeller. Föreliggande rapport beskriver metodiken för hur en 3-D diskret nätverksmodell kan konstrueras för bergmassasn närmast TBM tunneln. Syftet med projektet är att ta fram ett underlag för diskussioner angående bergstabilitet och grundvattenflöde i närområdet av deponeringstunnlar och kapselhål.

TABLE OF CONTENTS

1 INTRODUCTION

1.1 Background and objectives

The Äspö Hard Rock Laboratory provides excellent opportunities for measurements on fracture traces that can be used as input to numerical models. This project aims at producing a 3-D discrete fracture network (DFN) model of the rock mass proximal to the TBM tunnel in the HRL. The DFN model will serve as a platform for further exploration simulation regarding rock mechanics and ground water flow adjacent to deposition drifts and canister holes.

1.2 Fracture data

The modeling is based on geometrical data for 470 fractures mapped in TBM tunnel. These fractures are considered to be of a non-deterministic nature, i.e., they do not form a spatial pattern that meets the geological definitions of fracture zones used at Äspö. The information is compiled in the files *fracture.dbf*, provided by SKB, 1995-11-15, and *frac3d.dbf*, provided by VBB, 1995-12-19. In summary, the modeling considers geometrical information such as location, orientation and length. No distinction has been made on hydraulic properties, rock quality, rock genesis or geology. *Appendix A* describes how field data have been treated prior to storage in SKB's data base.

2 FRACMAN

FracMan is a name of a software package developed to model the geometry of discrete fractures. It provides an integrated environment for the entire process of statistical data analysis and stochastic modeling and partly consists of:

- statistical modules that allow for transformation of field data into the formats needed by FracMan for generating stochastic networks of discrete features,
- 3-D visualization to enhance the understanding of data gathered on 2D trace maps and 1D scan lines,
- exploration simulation tools to improve design and interpretation questions, and
- a Monte Carlo simulation tool to explore the uncertainty in the output due to the heterogeneity in the input (field data).

The integrated environment is illustrated in *Figure 2-1*. Section 2.1 gives a brief description of the FracMan modules FracSys and FracWorks. Section 2.2 discusses some limitations regarding stochastic fracture network modeling using FracMan.

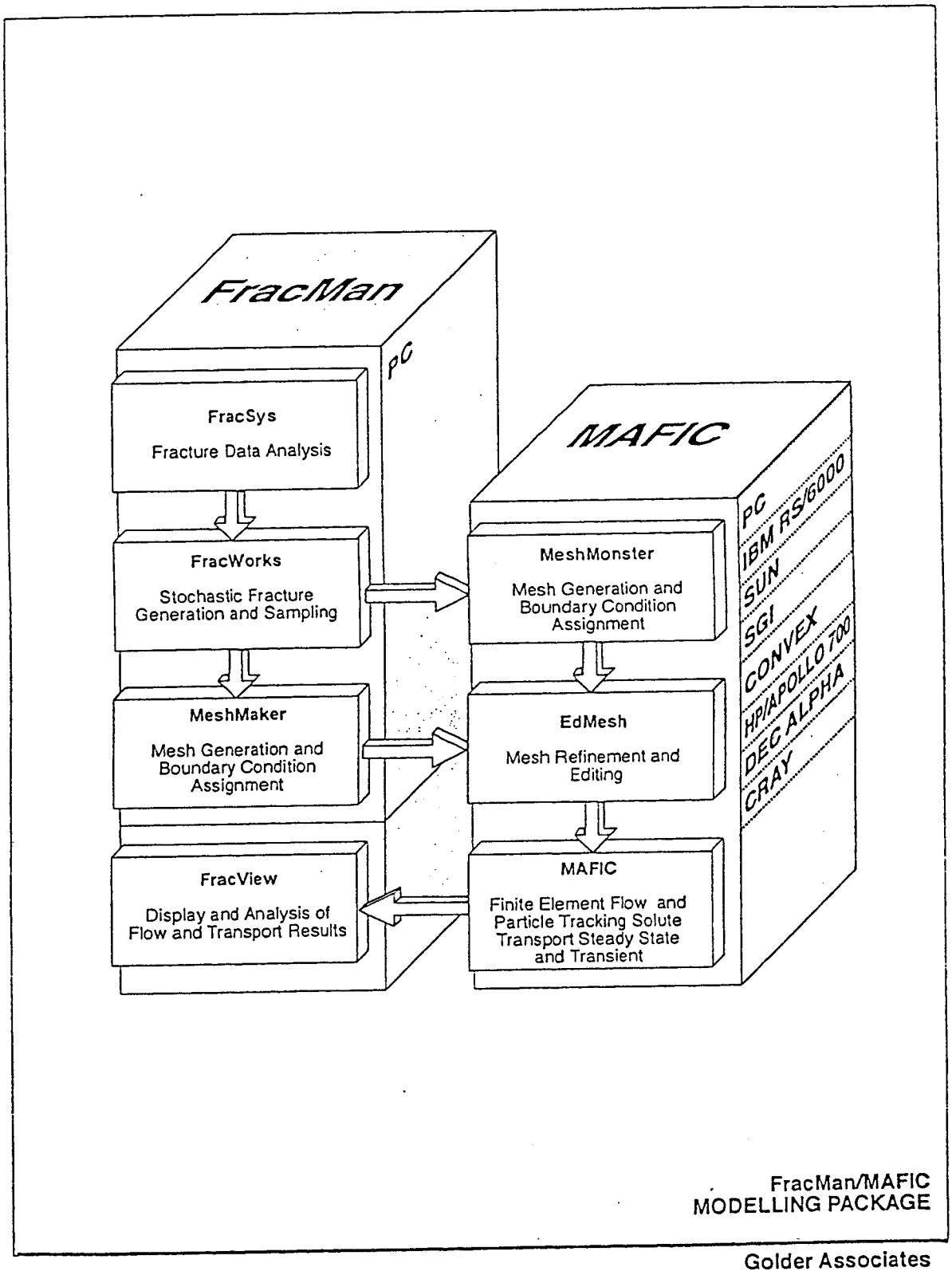

Figure 2-1 The integrated environment of fracture data analysis and modeling with FracMan as the discrete fracture network generator. MAFIC is a software package used for ground water flow and solute transport modeling.

2.1 FracSys

FracMan is useful for modeling possible geological conditions when there are little or no data. It is also useful for modeling in situ conditions when data are available. However, FracMan requires information in formats which are frequently not available as part of conventional data collection programs, although the information can be derived by appropriate procedures. *Table 2-1* summarizes FracMan input requirements and the FracSys modules used to derive the required information.

Table 2-1 *FracMan data requirements.*

FracMan Input Requirement	Raw Data	FracSys Module
Fracture Set Definition	Borehole Logs Fracture Trace Maps (Orientation, Infilling, Termination, Mineralization, Size, etc.)	ISIS
Fracture Set Orientation Distribution	Borehole Logs Fracture Trace Maps (Orientation)	ISIS
Fracture Set Termination Probability	Fracture Trace Maps	HeterFrac
Fracture Set Location Conceptual Model	Fracture Trace Maps (Trace Coordinates)	HeterFrac
Fracture Set Size Distribution	Fracture Trace Maps (Trace Length)	FracSize
Fracture Set Transmissivity Distribution	Packer Test Interval Transmissivities	OxFilet
Fracture Set Conductive Intensity	Packer Test Interval Transmissivities	OxFilet
Fracture Network Hydraulic Connectivity	Packer Test Transient Results	FracDim

2.2 FracWorks

FracWorks can generate a wide variety of discrete features from deterministic and/or stochastic descriptions, and show the results in a 3-D view on the computer screen. FracWorks realizations can be saved in different formats for further use in other programs dealing with exploration simulation, pathway analysis and ground water flow and solute transport modeling. Simplified exploration simulations and pathways analyses can also be carried out with FracWorks. For example, *Figure* 2-2 shows a FracWorks realization with 37 fractures in a $(20\ m)^3$ cube. The network is intersected by a horizontal deposition drift and a vertical canister hole. *Figure* 2-3 shows the trace map of the canister hole.

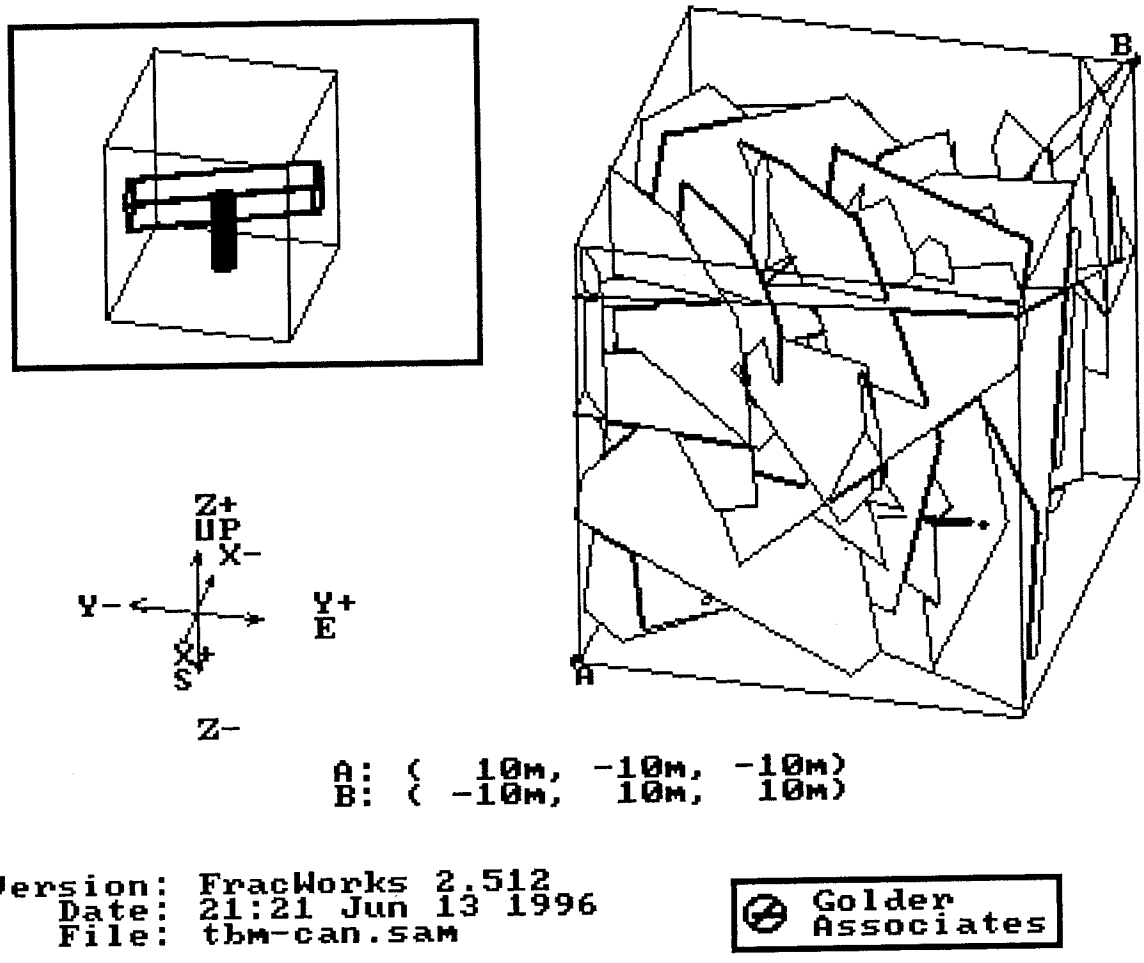

Figure 2-2 *FracWorks realization with 37 fractures in a* $(20\ m)^3$ *cube. The network is intersected by a deposition drift and a canister hole. Figure 2-3 shows the trace map of the canister hole.*

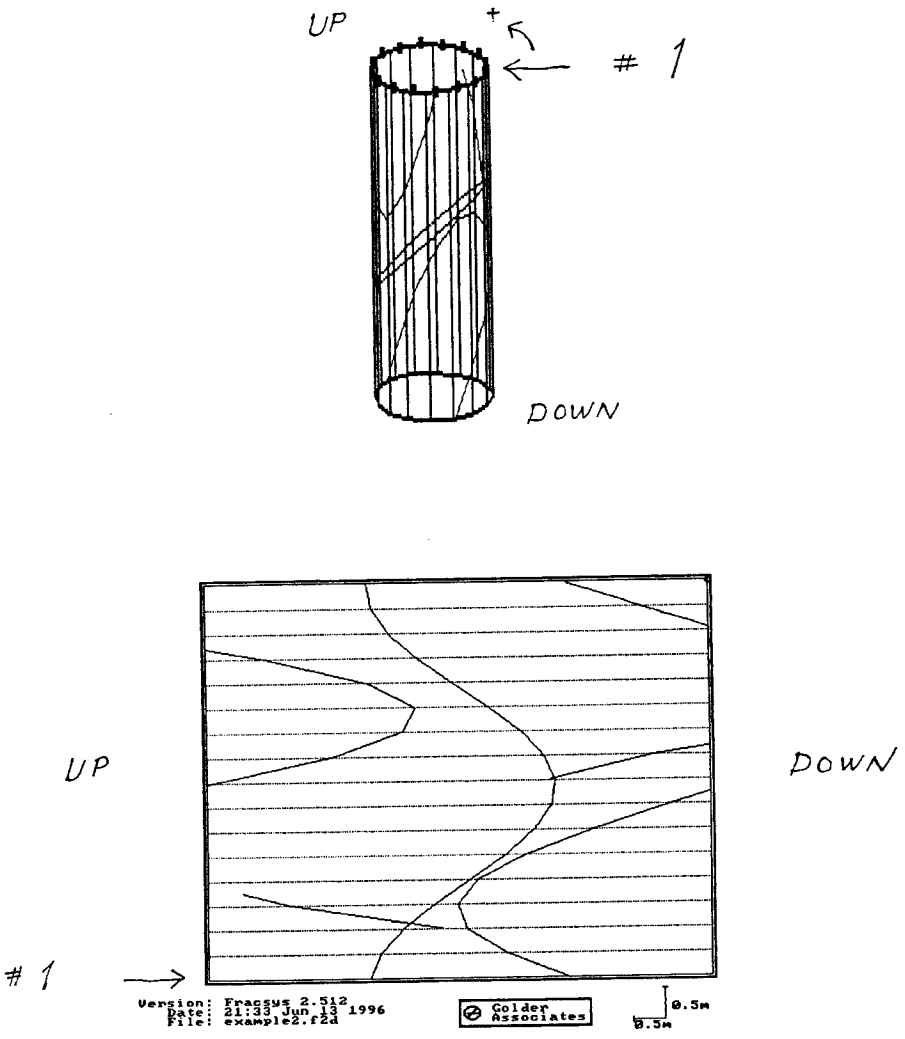

Tracy_00.sts created by FracWorks 2.512 21:26 Jun 13 1996 File: can-it.sam

==========

# of fracs in system : 37 P32: .494 sq.m2/cu.m
# of fracs connected to traceplanes: 5 # of traces: 5

Group:	# of Planes:	Planes:
1	16	1 2 3 4 5 6 7 8 9 10 11 12 13 14 15 16

Group	# of Fracs	# of [Xs, Ts, Ends]			Trace (m)
1	5	2	0	3	6.21

of [Xs+Ts]/sq.m = .3928E-01
of Frac / sq.m = .9820E-01
Termination prob. = .0000E+00
Termination pct = .0000E+00
Intensity (m/sq.m) = .6094E+00

Frac Stats	Mean	+- Std. Dev.	(Min,	Max)
Trace Length [m]	6.21E+00	+- 3.12E+00	(2.60E+00,	9.13E+00)

Figure 2-3 Trace maps and trace map statistics for the canister hole shown in Figure 2-2.

2.3 Limitations

Heterogeneities in field observations give rise to uncertainties, in particular when it comes to interpolation and extrapolation. Stochastic modeling uses statistics to describe observed heterogeneities, and Monte Carlo simulation (multiple realizations) to quantify the associated uncertainty. In this context, one should distinguish between unconditional and conditional simulation. FracMan is mostly used for unconditional simulation, which means that all realizations correctly reproduce the inferred statistics of the observed fracture traces although the exact locations of the simulated traces may be incorrect. Unfortunately, the large amount of data that is treated when dealing with discrete fractures imposes severe computational constraints. In general, it is difficult to apply conditional simulation in fractured rocks.

Stochastic models are useful for interpolation and extrapolation problems in heterogeneous media. Depending on the nature of the heterogeneities different degrees of procedures may be used to make field data satisfy the assumption of statistical stationarity. Statistical stationarity means that the statistical moments (mean, variance,...) are stationary in space, i.e., independent on the location. Whether statistical stationarity can be assumed without any further treatment is a question that has to be answered form case to case. In summary, the validity of a stochastic DFN model is governed by:

- scale of observation
- methods of data collection (i.e. truncation, degree of detailing)
- outcrop size (i.e. underground, surface)
- outcrop type (i.e. blasted tunnel, bored tunnel, boreholes)
- instrument limitations (i.e. hydraulic the test equipment resolution threshold)

3 ANALYSIS OF FRACTURE DATA FROM THE TBM TUNNEL

Geometric analyses have been carried out on the TBM tunnel data set and consider orientation, size, spatial pattern and intensity. *Figure 3-1* shows the scheme used for the analysis.

A discussion regarding the statistical stationarity of the TBM tunnel data set is presented in Section 3.1. Section 3.2 describes the analysis of fracture orientations. Section 3.3 summarizes the iterative process of determining a fracture size distribution. Section 3.4 treats the calculations of fracture intensity. Finally, Section 3.5 deals with the spatial distribution of fractures. The resulting model is presented in Section 3.6.

3.1 Statistical stationarity

Before a stochastic model is constructed it is important to study the input data regarding statistical stationarity. If the statistical moments of the analyzed data are dependent of location within the modeled rock volume there are two options: use a non-stationary description, or divide the modeled volume into subregions that are locally stationary but globally non-stationary. FracMan can handle both cases.

The circular perimeter of the TBM tunnel is approximated in this report by a hexagon. *Figure 3-2* shows a projection of the real trace maps from the three straight segments of the TBM tunnel onto the corresponding hexagons. That is, each trace has been projected onto a hexagon that is located inside the TBM (i.e. the vertices of the hexagon touch the perimeter). As indicated in *Figure 3-2*, the fracture intensity measure P_{21} (m of fracture length/m^2 of trace plane area) increases slightly from 0.546 m/m^2 for Segment 1 to 0.656 m/m^2 for Segment 3.

The slight change of P_{21} in *Figure 3-2* refer to an observation scale of 100-200 m. In order to study whether trace data are dependent on location, P_{21} on a smaller scale must be calculated. The values shown in *Figure 3-3* have been calculated by dividing each segment in *Figure 3-2* into 20 m long subsegments. The variation of P_{21}-20m is obvious, however, it is difficult to be conclusive whether there is a clear trend. *Figure 3-4*, which shows the P_{21}-Mean and P_{21}- Std. dev. as a function of the "observation scale", suggests that a stationary model is probably appropriate. For the purpose of this study a P_{21}-value of 0.546 was chosen as the mean intensity value for the desired DFN model.

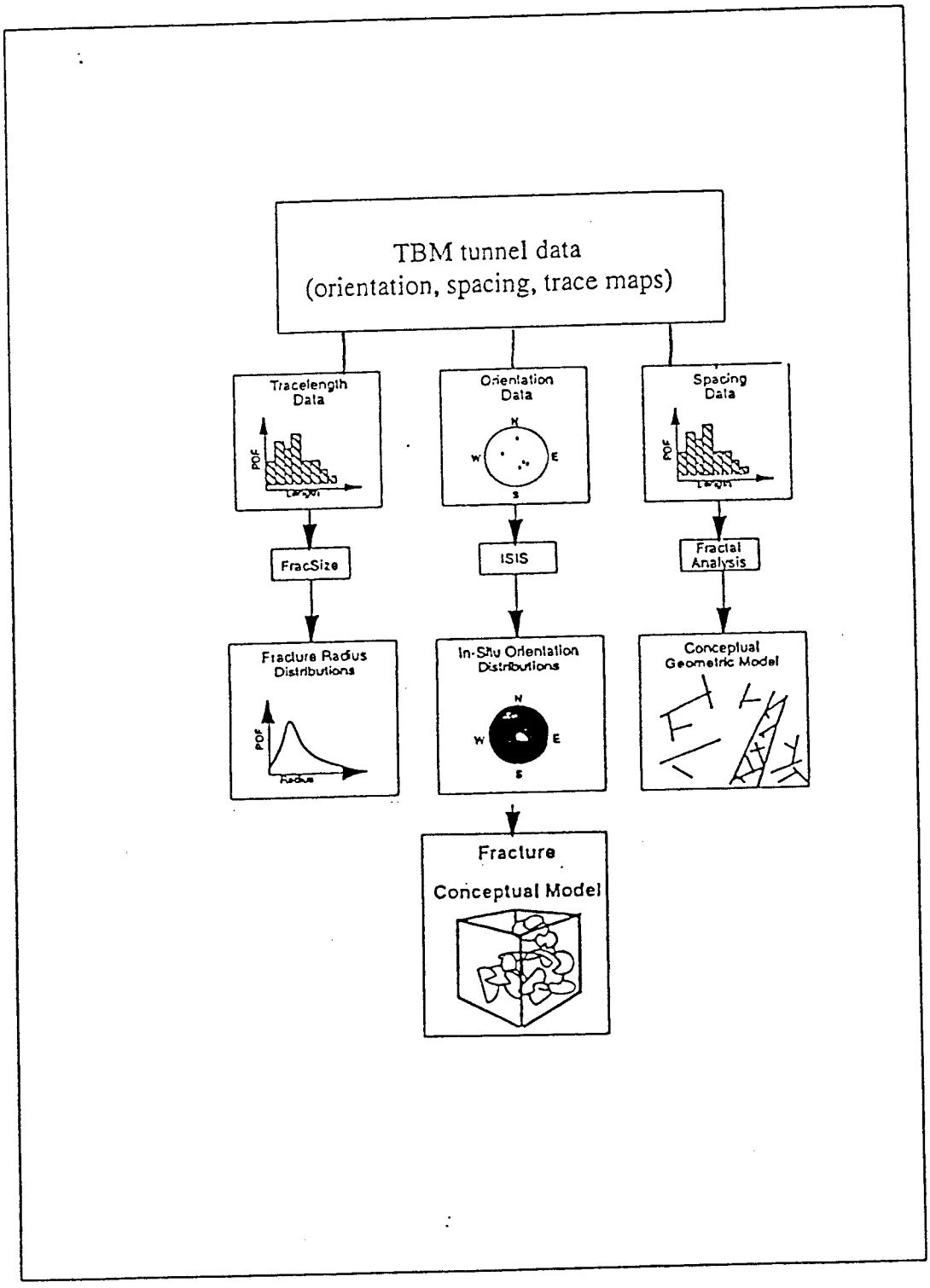

Figure 3-1 Scheme of analysis of fracture data used for the development of a discrete fracture model of the TBM rock mass.

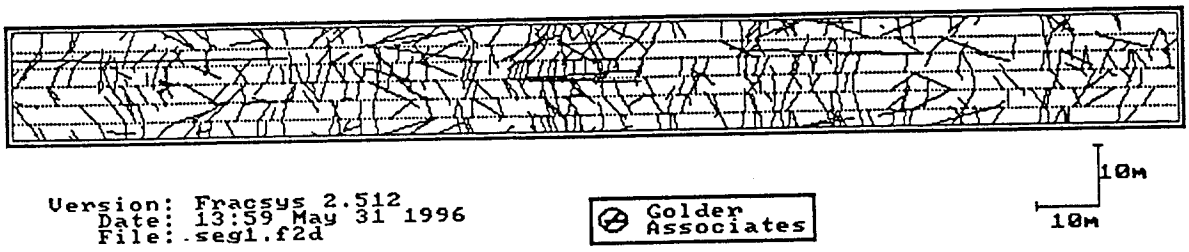

Segment 1

Center line characteristics: L =189.97 m, Trend = 259.86, Plunge= 8.25
$x_{\bar{A}}$ = 2,268.829, $y_{\bar{A}}$ = 7,308.707, $z_{\bar{A}}$ = –418.23
P_{21} = 0.546 m/m^2

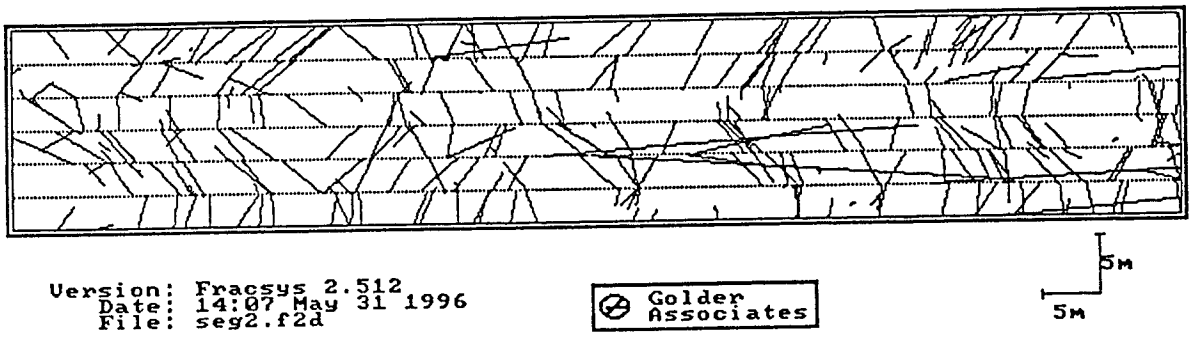

Segment 2

Center line characteristics: L =99.83 m, Trend = 262.35, Plunge= 1.31
$x_{\bar{A}}$ = 2,083.759, $y_{\bar{A}}$ = 7,275.617, $z_{\bar{A}}$ = –445.49
P_{21} = 0.558 m/m^2

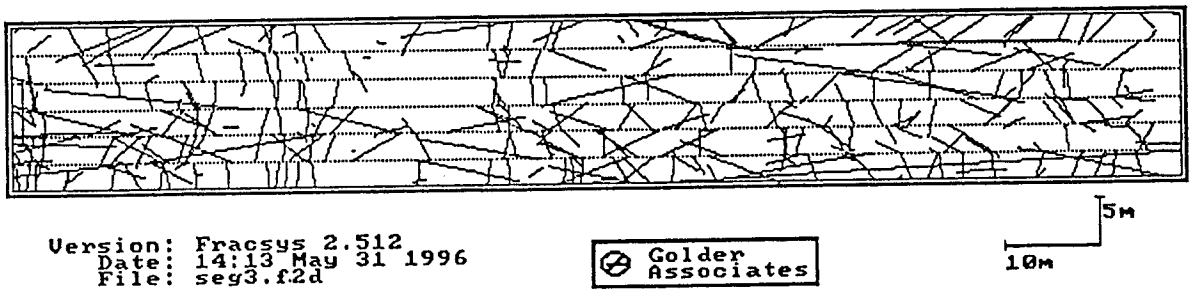

Segment 3

Center line characteristics: L =122.03 m, Trend = 277.16, Plunge= -0.94
$x_{\bar{A}}$ = 1,984.84, $y_{\bar{A}}$ = 7,262.33, $z_{\bar{A}}$ = –447.768
P_{21} = 0.656 m/m^2

Figure 3-2 Trace maps of the three TBM segments with observed P_{21}-values. Note the differences in scale.

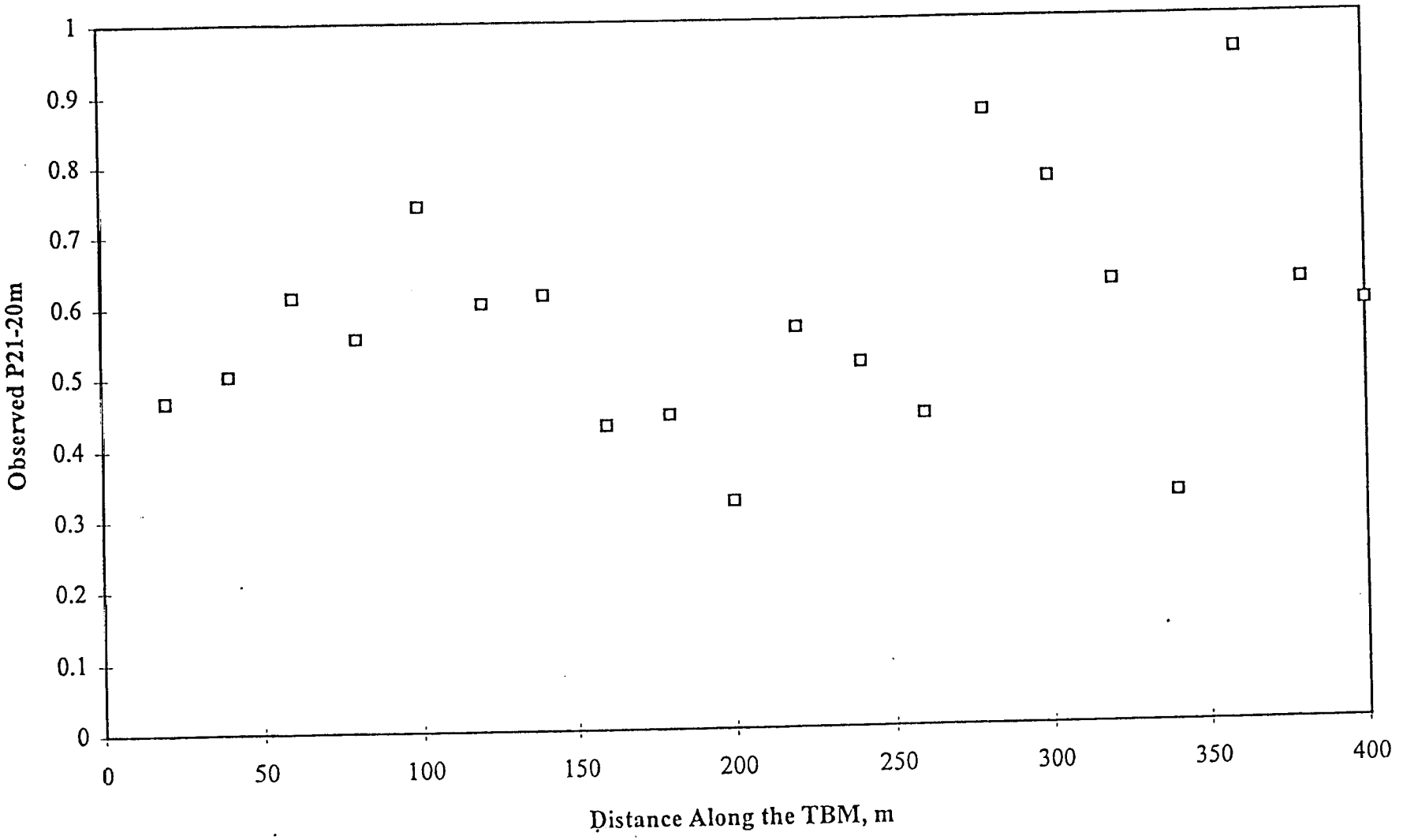

Figur 3-3 Observed P_{21}-values in 20m intervals. Mean P_{21}-20m for 0-200m is 0.529. Mean P21-20m for 0-400m is 0.578.

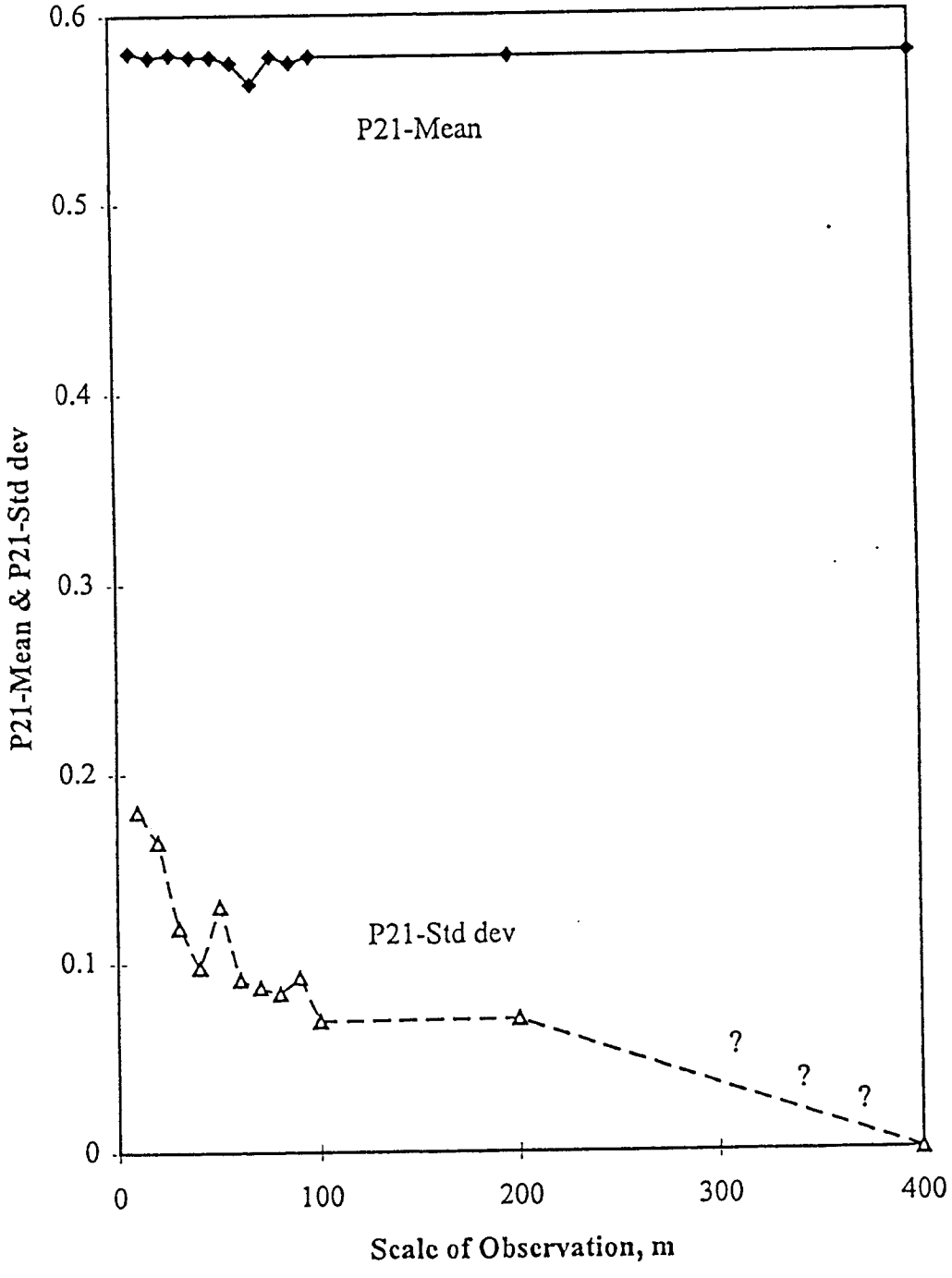

Figure 3-4 TBM P_{21} statistics; mean and standard deviation vs. scale of observation.

3.2 Orientation

The separation of fractures into different sets can significantly improve the performance of a DFN model. Fracture sets can have different properties assigned to them providing more realistic models. Previous studies of Äspö HRL tunnel data (La Pointe et al., 1995; Munier, 1993, 1995) have put great efforts in statistically separating fractures into sets based on fracture mineralogy, orientation, trace length, termination modes, surface roughness, kinematical evidence etc. The main results show that there is no or very weak correlation of most fracture properties, with the exception of a slight increase in the trace length for water bearing fractures. Selective fracture orientation has proven earlier to be of significant help in distinguishing major water bearing fractures throughout the Äspö HRL (Hermanson 1995), where typical water bearing faults tend to be steeply trending NW to NNW. Within the scope of work of this project there has been taken no account to hydraulic aspects while constructing a DFN model of the TBM rock mass.

An attempt has been made to extract fracture sets by orientation. The discriminant analysis has been kept strictly statistical, to avoid subjective bias as far as possible. The inferred sets have then been statistically analyzed within the FracSys module ISIS (see *Table 2-1*).

Figure 3-5 shows an equal area stereo plot (Schmidt net) of the 470 fractures in the TBM tunnel. The dots represent fracture poles and the Schmidt net show the poles' orientation in space. Three fairly clustered fracture sets can be depicted by this figure; one sub-horizontal fracture set and two vertically dipping sets with NW and ENE trends.

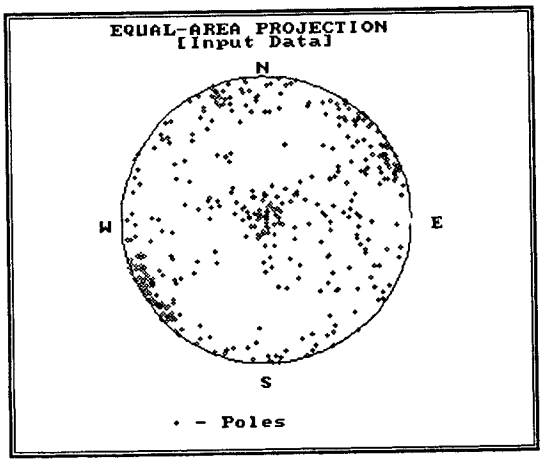

Figure 3-5 Schmidt net of the 470 fracture poles.

The three sets were tested statistically for a number of different orientation distributions, see *Figure 3-6*. *Table 3-1* summarizes the goodness-of-fit for how well a Fisher orientation distribution fits each set. The K-S value reported in *Table 3-1* is the Kolmogorov-Smirnov test statistic followed by its percentage of significance. As shown the Fisher model is a poor representation for two of the three sets. Subsequent analyses with other orientation distribution models (Normal, Bingham, Bivariate) show similar results. For this reason, the orientations of the fractures in the constructed DFN model were bootstrapped directly from the stereo plot of the fracture orientations in *Figure 3-5* rather than generated from a statistical model for distributions of point on a sphere, such as the Fisher distribution.

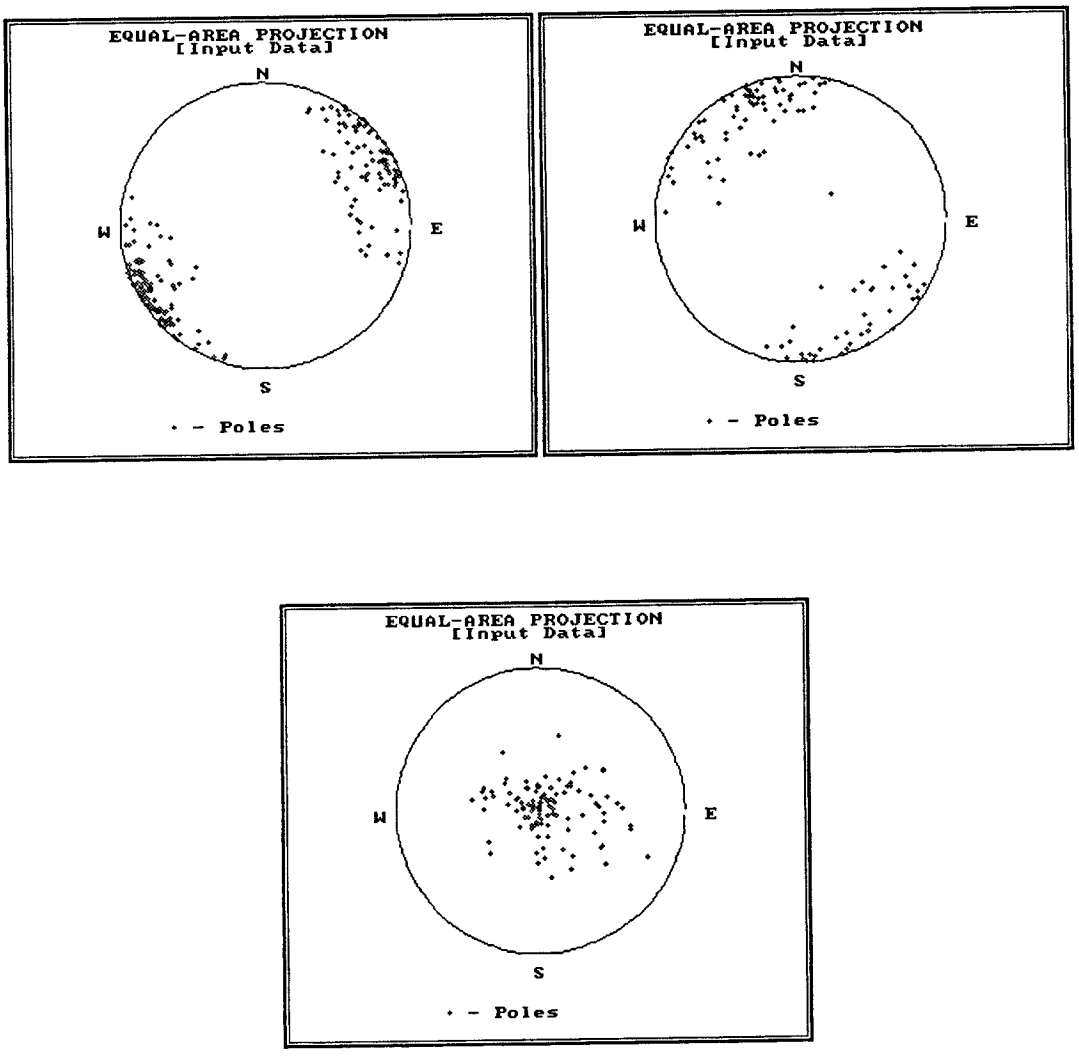

Figure 3-6 Three possible sets of fractures.

Table 3-1 Kolmogorov-Smirnov goodness-of-fit results for the Fisher distribution.

Set	Distribution	Mean Pole (Trend, plunge)	Major Axis (Trend, plunge)	Dispersion	K-S (value,% of sign)	% of fractures
All		232.6, 11.7	52.6,78.3			100
Set 1	Fisher	58.7, 1.8	238.7, 88.2	13.37	0.136, 0.05	48.1
Set 2	Fisher	334.2, 5.6	154.2, 84.4	7.82	0.045, 96.7	25.7
Set 3	Fisher	71.7, 85.8	251.7, 4.2	11.92	0.146, 1.1	26.2

3.3 Fracture size

Fracture size is an important component of a fracture network. *Table 3-2* provides statistics for fracture traces in the TBM tunnel. A histogram of the fracture trace lengths is shown in *Figure 3-7*.

Table 3-2 Trace statistics for fractures in the TBM tunnel.

	SICADA TBM data
TBM tunnel length	411.83 m
Approx. Mapped area	12938 m^2
Number of traces	470
Total trace length	2461.4 m
Mean of trace length	5.24 m
Median of trace length	4.75 m
Std dev of trace length	4.17 m
Variance of trace length	17.38 m
Min trace length	1.3 m
Max trace length	55 m
Approx fracture intensity P_{21}	0.55 m^{-1}

Fracture size can not be derived directly from fracture trace length, because of the severe censoring caused by the insufficient size of the tunnel with regard to the fracture area. LaPointe *et al.* (1993) showed that when fractures are larger than the tunnel cross section, the distribution of trace lengths that would be observed on tunnel walls can yield the same statistics even for quite different fracture size distributions. Thus, trace length distributions where many traces are censored are not useful for inferring fracture size. However, LaPointe *et al.* (1993) also showed that the censoring effect itself can be used to estimate fracture size from fracture traces.

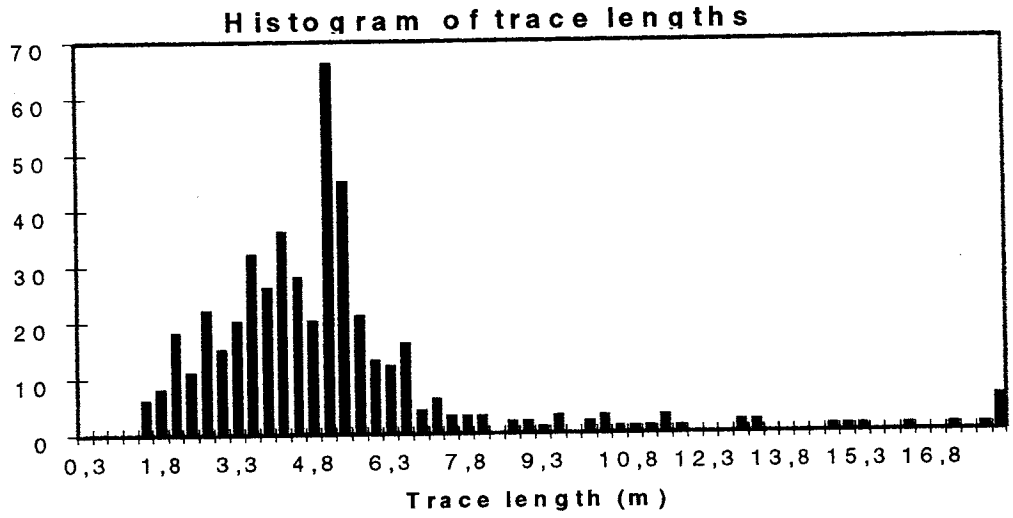

Figure 3-4 Histogram of mapped trace lengths in the TBM tunnel.

In short, LaPointe *et al.* (1993) showed that for a particular fracture orientation, tunnel orientation and tunnel cross-section, the probability that a fracture trace could be mapped all the way around the tunnel surfaces is a function of fracture size. By computing the statistics for the amount of the tunnel surface that traces for a particular fracture set occur on, it is possible to estimate the fracture size[1] distribution.

For the purpose of this project the TBM tunnel surface was divided into six panels and the amount of tunnel surface that each fracture intersected in terms of percentage of panel intersections was computed. To derive a fracture size distribution, a series of simulations were carried out for a range of different fracture size distributions. The procedure for this analysis utilizes FracMan to generate a number of realizations and perform simulated exploration with a hexagonal drift in the stochastic model. From the trace maps of the tunnel panel intersections of the simulated fracture traces the optimal fracture size distribution was determined. The simulated drift has identical measures as the real TBM tunnel. To improve the quality of the statistics 30 realizations for each size distribution were carried out.

Earlier studies of fracture size, both at Äspö and elsewhere indicate that fracture size follow a lognormal distribution (LaPointe *et al.*, 1995). Where there are several combinations of mean and standard deviation that produce the same intersection statistics, distributions with a very small standard deviation are geologically improbable as this implies that the fracture size distribution is close to uniform.

[1] It should be noted that FracMan uses fracture radius as a surrogate for fracture size.

There is no published evidence that fractures are of nearly uniform size. On the contrary, published trace maps show a wide range of trace lengths, suggesting that fracture sizes may vary widely. For the determination of the most appropriate fracture size distribution in this project, the following two-step procedure was used:

- Investigate a range of possible log-normal size distributions with different means and a constant valued standard deviation.
- Using the best mean value(s), investigate a range of different standard deviations and choose the best. If several distributions are equally good, choose the size distribution that has the maximum standard deviation.

The parameters for log-normal distributions are given in arithmetic space in FracMan. For the interested reader, *Appendix B* explains how the transformations to logarithmic space are done.

In total for this analysis, 26 × 30 (780) realizations of the TBM rock mass with 20,000 fractures each, were generated. For the first 15 sets of 30 realizations the standard deviation was kept constant valued (1 m) whereas the mean varied between 4 m and 18 m. For the remaining 11 sets, the mean value was kept more or less constant valued while the standard deviation was altered between 1 and 5.

Sampling was made in each realization (780 times) using a simulated TBM tunnel and the percentage of panel intersections with the fracture traces were calculated. The result is plotted in *Figure 3-8*. The dashed lines in *Figure 3-8* represent the observed panel intersections of the mapped fractures in the TBM tunnel. *Figure 3-9* provides a simplified graph of the information in *Figure 3-8*. In conclusion, *Figure 3-8* and *3-9* show that fracture size distributions with a mean radius of 6 to 8 m fits the observed intersection statistics pretty well.

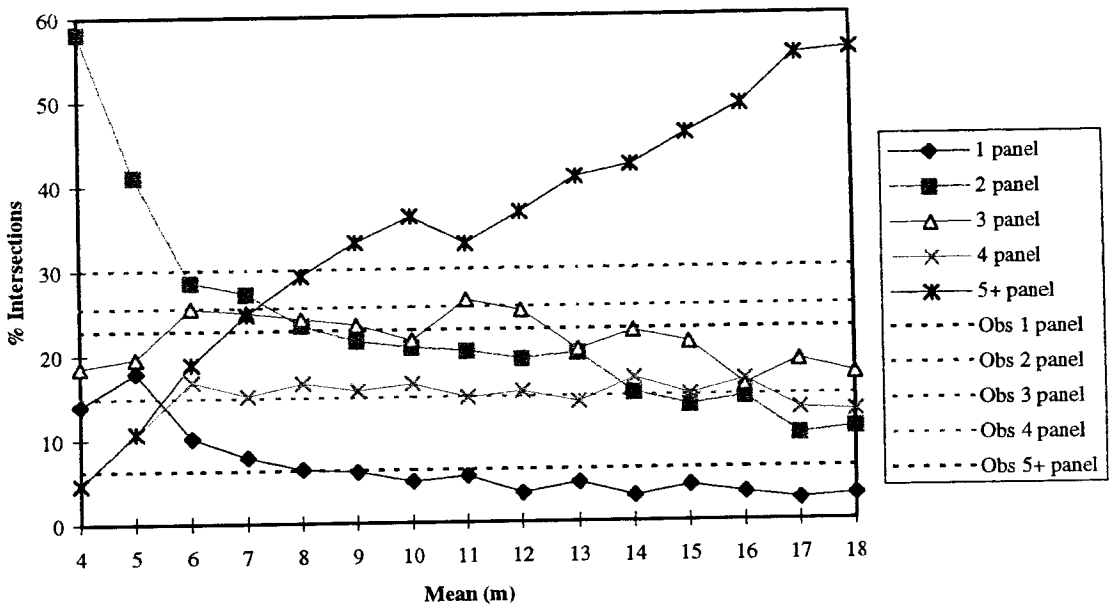

Figure 3-8 Panel intersection statistics of simulated size distributions with varying means (4 - 18 m) and constant valued standard deviation (1 m).

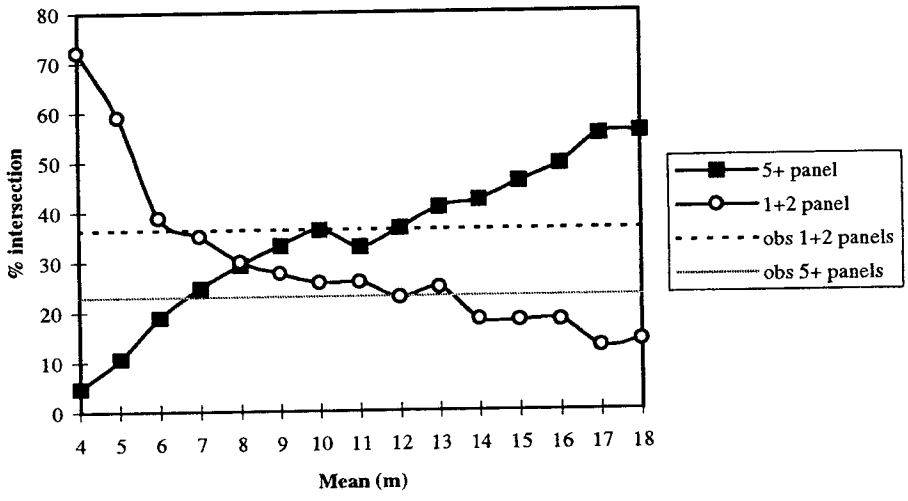

Figure 3-9 Simplified graph of the information shown in Figure 3-8 with summarized intersections of panel 1 & 2 respectively panel 5 & 6.

Figure 3-10 presents fracture size distributions where the mean varies between 6 and 10 m and the standard deviation varies between 1 to 5 m. This figure shows the relative difference (divergence) between simulated and observed panel intersection statistics for different fracture size distributions. For the purpose of this report, the match correspoding to a log-normal fracture size distribution with a mean of 6 m and a standard deviation of 3 m was chosen for the desired DFN model.

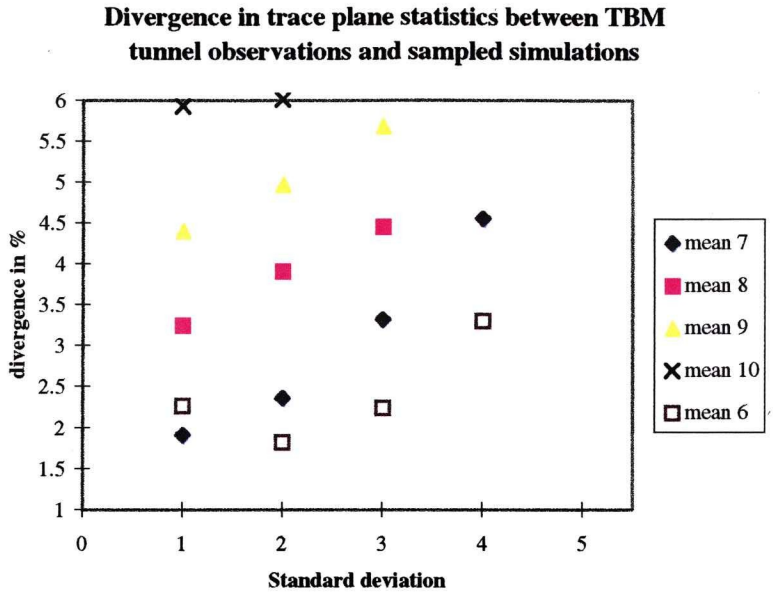

Figure 3-10 *Relative difference (divergence) between simulated and observed TBM trace map intersection statistics.*

3.4 Intensity

Fracture intensity is defined as the amount of fracture area per unit volume rock (m^2/m^3). In FracMan this entity has the symbol P_{32} . P_{32} is directly proportional to the number of fractures intersecting a borehole, P_{10} , and to the trace length per area unit on an outcrop surface, P_{21} . However, both P_{10} and P_{21} depend upon the orientation distribution of the fractures. They also depend on the fracture size and the shape of the borehole or sampling plane. P_{32} , however, does not depend on how many fractures there are, nor on the size distribution (Dershowitz & Herda, 1992).

The fracture intensity measure P_{32} cannot be measured directly in the field. However, applying its linear relationships with P_{10} and P_{21} , P_{32} can be calculated from tunnel trace maps or borehole intersection frequency. The way to do this is to generate a fracture network with a hypothetical P_{32} with bootstrapped orientation data. Note that P_{32} is independent of the exact fracture size distribution so at this stage a generic fracture size distribution can be used. 30 realizations are generated and simulated P_{21} values are calculated through sampling with a simulated tunnel drift, equivalent in size and orientation to the mapped TBM tunnel. The ratio of the prescribed P_{32} value for the simulation, $P_{32,sim}$, and the simulated P_{21} value, $P_{21,sim}$, is then multiplied by the observed $P_{21,obs}$. The result provides an estimate of the true P_{32} in the real TBM tunnel,

$$P_{32} = P_{32,sim} (P_{21,obs}/P_{21,sim})$$

For the purpose of this project, the analysis of P_{32} was carried out by creating an experimental fracture network model, see *Table 3-3*. The observed P_{21} is 0.546 in the first segment of the TBM tunnel. Mean of $P_{21,sim}$ from trace maps along the simulated TBM drift is 4.08. The fracture intensity P_{32} for the TBM is then computed as

$P_{32} = 3.5\ (0.5459/4.08) = 0.47\ m^{-1}$

Table 3-3 DFN model used for the P_{32} calculations.

Spatial model	Enhanced Baecher
Fracture size distribution	Log-normal, m=6 m and s = 3 m
Orientation distribution	Bootstrapped
Simulated $P_{32,sim}$	3.5
Model size	(50 × 50 × 50) m^3
Estimated number of fractures/ realization	3700
Number of realizations	30

It should be noted that the derived P_{32}-value is based on the P_{21}-value of Segment 1 of the TBM tunnel. We know from *Figures 3-3* and *3-4* that observations on different scales give approximately a constant-valued P_{21}-Mean.

The derived P_{32}-value of 0.47 in this report can be compared with the P_{32}-values reported in previous works dealing with Äspö HRL data. For example, LaPointe *et al.* (1995) computed a P_{32}-value for the conductive fractures (P_{32t}) in the Äspö HRL of about 0.33 m^{-1}. Uchida *et al.* (1994) used 3 m and 30 m packer tests to estimate the conductive P_{32} to be about 0.0664 m^{-1}. Dershowitz *et al.* (1996) concluded that flow logs and packer tests in KXTT boreholes in the TRUE volume imply a conductive P_{32}-value between 0.5 to 2.0 m^{-1} for fractures with transmissivities greater than 10^{-9} m^2/s.

The differences in the reported values for the conductive P_{32} may be caused by, for example, the following factors:

- differences in the way the used tunnel excavation methods affect the rock
- differences in the scale of observation (borehole, tunnel, outcrop)
- mapping methods (truncating, censoring)
- measurement equipment (cores, TV-logs, flow logs)

It is likely that conventional blasting and excavation creates additional fractures and enlarges existing ones in the vicinity of the tunnel. Also, the scale of observation may induce a severe bias at the mapping stage. For instance, core logging includes fracture sizes below the truncation of fractures in the tunnel. Further, the smooth surface of the TBM tunnel surface may make it difficult to observe fractures with low relief.

Likewise, it is easier to recognize conductive fractures by the fact that they are wet. Fracture intensity estimates from hydraulic tests may be significantly affected by the test equipment resolution threshold. Scale of observation is relevant also in hydraulic estimates of the fracture intensity.

3.5 Spatial model

It is generally believed that trace maps provide information about the intensity and the spatial distribution of fractures within the three dimensional rock block. One of the more common spatial models is the Baecher model, which uses a Poisson point process for generating fracture centers in space. Another common model is the BART model, which extends the Baecher model by providing a possibility to allow for fracture terminations. *Figure 3-11* shows the spatial models that are available in FracMan.

The determination of which spatial model that is most appropriate is accomplished in FracMan by means of statistical tests and geometrical measures such as the χ^2-test and the box fractal dimension. For example, a χ^2-test can be used to compare the observed distribution of fracture centers to a theoretical Poisson distribution. A significance of 85% or greater generally indicates a good fit to the Poisson distribution and a high probability that the Beacher model is appropriate. The box fractal dimension is a measure of how completely the fracture pattern fills the trace plane surface. A fractal dimension near 1 indicates a very strongly clustered, heterogeneous pattern, whereas a dimension close to 2 indicates a more homogeneous, space filling pattern. Large fractal dimensions indicate Poisson type models whereas smaller dimensions indicate clustered models such as the Nearest neighbor , War zone or Levy-Lee fractal models.

A spatial analysis of the trace maps from the TBM indicates that a Poisson distributed model for the observed data is appropriate. *Figure 3-12* shows that the significance level is 99% for the χ^2 -test. The box fractal dimension is 1.925, which suggests a homogeneously space filling pattern of the fracture traces.

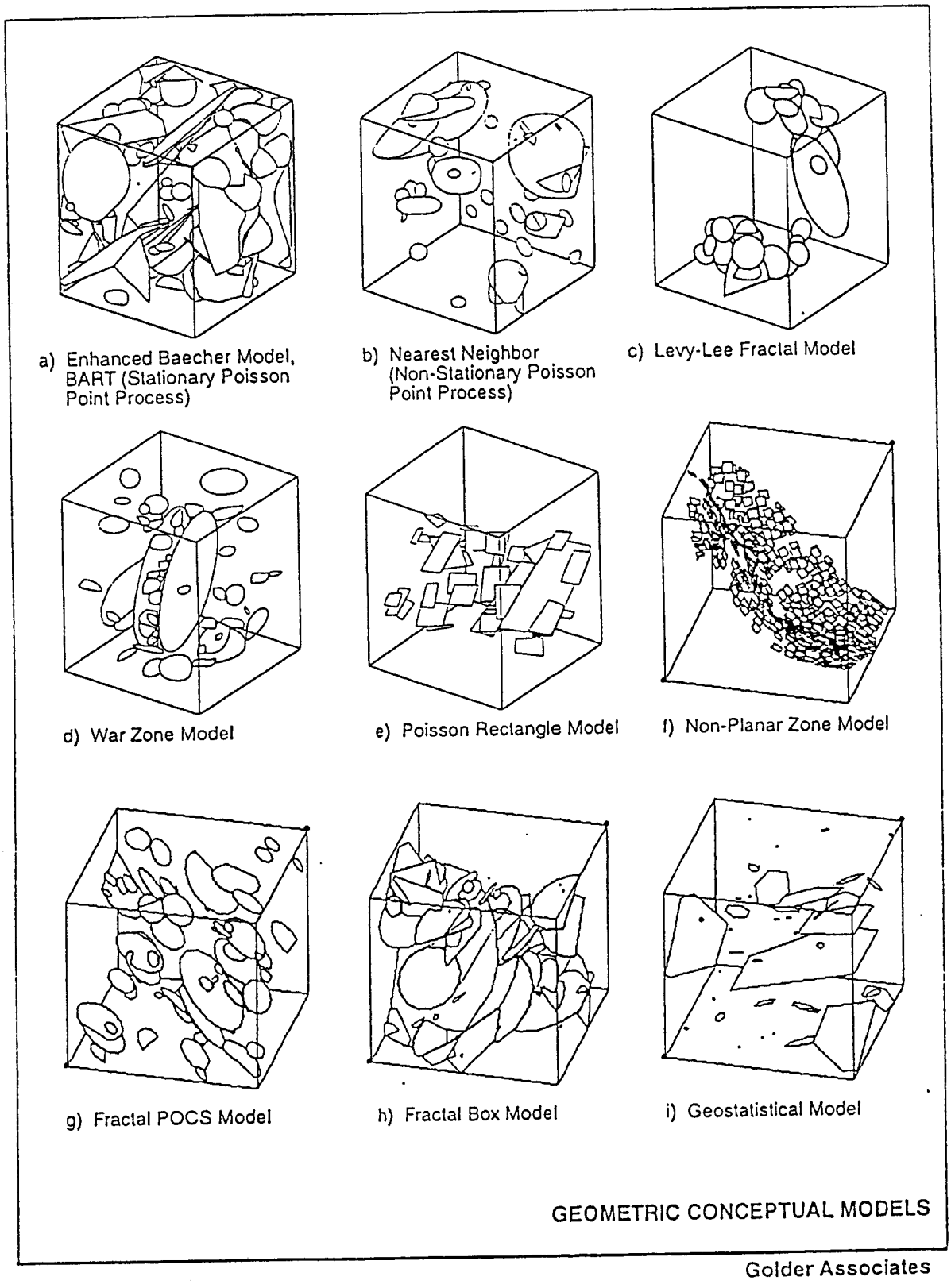

Figure 3-11 Example of geometric models used in FracMan for modeling the 3-D spatial distribution of fractures.

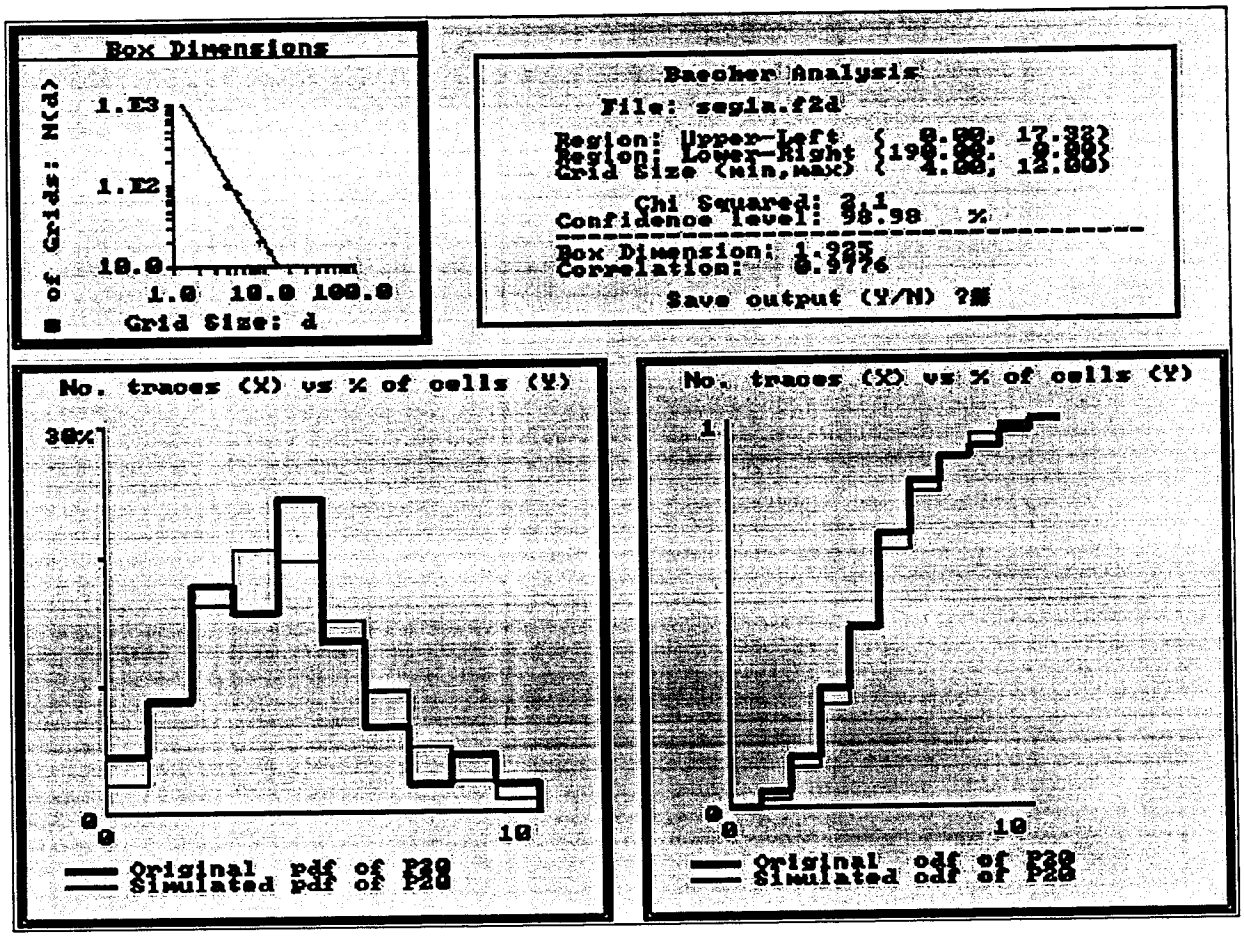

Figure 3-12 A spatial analysis of the trace maps from the TBM suggests that a Poisson distributed spatial model with a homogeneous space filling may be appropriate

3.6 Summary

Table 3-4 presents the calculated parameters for the TBM DFN model. The modeled domain is cylindrical with a radius large enough to cover implementation of canister holes.

Table 3-4 Parameters of the inferred DFN model of the TBM rock mass using FracMan.

Location model	Baecher
Orientation distribution	Bootstrapped from TBM *fracture.dbf* data, Fischer dispersion = 300
Fracture size distribution	Log-normal, m = 6 m, s = 3 m
Fracture intensity P_{32}	P_{32} = 0.47
Model size	Cylindrical with L= 220 m , R = 25 m

4 VERIFICATION OF THE DFN MODEL

4.1 Verification using P_{21}-20m values from the TBM tunnel

Figure 3-3 shows the P_{21}-20m values along the entire TBM tunnel. The P_{21}-20m values between 0 and 200 m are of particular interest here as these values coincide with the first segment of the TBM tunnel. The question asked here is if the inferred DFN model, which is calibrated to match the P_{21}-value of Segment 1, can be used on much smaller scale. For example, can the inferred DFN model reproduce the heterogeneity of the TBM rock mass on a 20 m scale as described by the variability of the observed P_{21}-20m values? If this is the case, then we may conclude that 1) the TBM tunnel data set may support the assumption of statistical stationarity (see *Figure 3-4*), and 2) the inferred model may meet the requirements for future near field exploration exercises.

In order to answer the above question, the inferred DFN model was used to generate 30 realizations of a $(20\ m)^3$ cube. Each cube was sampled with a simulated tunnel and the P_{21}-value for the intersecting fractures was calculated from the trace maps. The simulated tunnel had the same dimension and orientation as the first segment of the TBM tunnel

Secondly, the 30 realizations were divided into three sets, where Set 1 corresponded to realizations 1-10, Set 2 to realizations 11-20 and Set 3 to realizations 21-30, respectively. The P_{21}-values of each set was then arranged in ascending order. So was the 10 first P_{21}-20m shown in *Figure 3-3*.

Finally, the values of each set were plotted versus the observed P_{21}-values. *Figure 4-1* shows the cross plot with the simulated P_{21}-20m values on the ordinate and the observed P_{21}-20m value on the abscissa. The cross plots suggests a good agreement.

4.2 Verification using borehole KA3191F

Borehole KA3191F was drilled prior to the TBM tunnel in a sub-parallel direction to the TBM tunnel. KA3191F was more than 200 m long and the core analysis showed 593 fracture intersections, rendering a fracture frequency close to 2.8 fractures per meter.

Simulated sampling of a synthetic borehole through the TBM DFN model was performed with the same orientation, length and borehole diameter as KA3191F. The results after 30 realizations of the model show that the model produces fracture frequency about seven times lower than observed in KA 3191F.

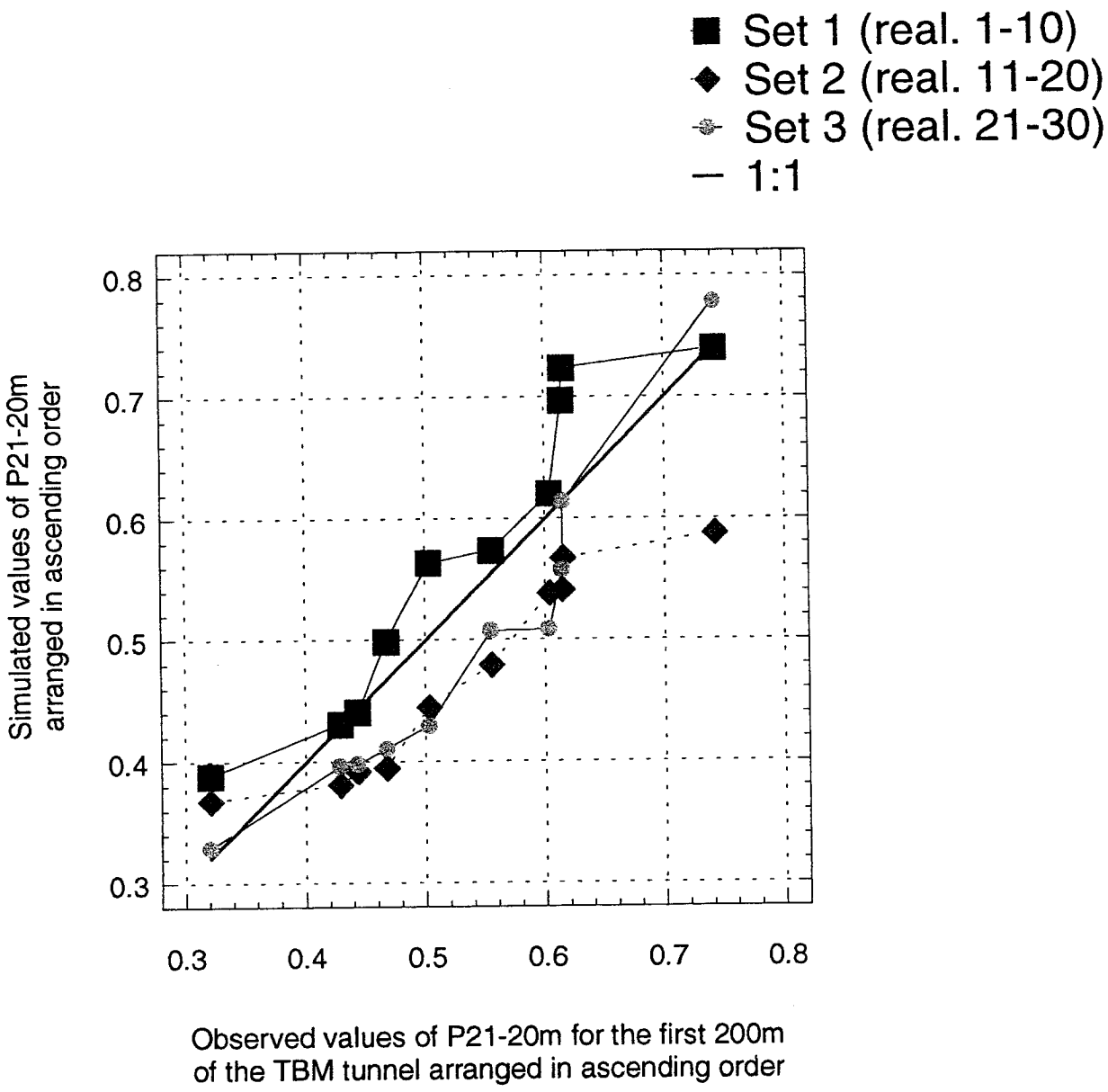

Figure 4-1 *Simulated P21 vs. observed P21 in the TBM tunnel. The data values in each set are arraged in ascending order.*

In conclusion, the inferred DFN model cannot reproduce the core statistics of KA3191F. However, it should be noted that the significant difference in the results can partly be attributed to:

- differences in the scale of observation
- differences in the mapping resolution
- differences between core analysis and trace map analysis

The tunnel mapping was deliberately subjected to a truncation threshold of 1 m, whereas all fractures intersecting the core were mapped without any threshold. Already this would give significantly different fracture frequencies between borehole and tunnel depending on the proportion of fractures with size less than a meter. Also, the amount of artificial fracturing in a drill core is substantial, and significantly contributes to the increased fracture frequency. Based on the experience from a large number of boreholes and tunnel information throughout the Äspö HRL, Stanfors (1996) notes that the average fracture frequency in drill cores is about four to five times higher than in the tunnel. Also Dershowitz *et al.* (1996) concludes that depending on the source of data the fracture frequency changes. *Table 4-1* shows some observations of fracture frequency, P_{10}, from different sources.

Table4-1 *Observations of typical fracture frequencies for different sources in the Äspö HRL.*

Source	*Type of fracture*	*Fracture frequency P_{10}, m^{-1}*
Drillcore logging	All fractures	2-6
Borehole TV (BIPS)	All fractures	0.5-2.4
Blasted tunnel (scanline)	All fractures	0.4-0.7
TBM tunnel (scanline)	All fractures	0.2-0.4
Flow logs	Conductive fractures	0.1-0.2

Table 4-1 implies that a DFN model constructed from data originating from one type of source is generally not possible to verify using data from another type of source, unless the degree of difference between the two types of sources is well known.

5 EXPLORATION SIMULATION

For the purpose of this project, the inferred DFN model was used to generate 30 realizations of a $(20\ m)^3$ cube. Each cube was intersected by a horizontal drift and a vertical canister hole similar to *Figure 2-2*. *Figures 5-1* to *5-5* show condensed statistical information from the 30 realizations. Based on the information in these figures an excerpt of the canister trace maps for the 30 realizations is shown in *Appendix C*, namely canister trace maps for realizations 1 to 9 and realization 30.

Figure 5-1: No. of Block Fractures & No. of Canister Holes Traces for each realization.
The figure suggests that the number of fractures in a 20 m cube varies between 26 and 58 and that the number of traces in a canister hole varies between 1 and 7.

Figure 5-2: No. of Canister Hole Traces & Crossings for each realization.
The figure shows which realizations that have large number of trace crossings.

Figure 5-3: Canister Hole Trace Crossings vs. P_{21}-CAN.
The figure raises the question whether P_{21}-CAN could be used as a simple measure to discriminate a given canister holes from a mechanical viewpoint.

Figure 5-4: P_{21}-TBM and P_{21}-CAN for each realization.
This figure shows that P_{21}-TBM cannot be used to predict P_{21}-CAN.

Figure 5-5: P_{21}-CAN vs. P_{21}-TBM.
This figure shows that the variability of P_{21} is scale dependent. and perhaps not normally distributed for small observation scales.

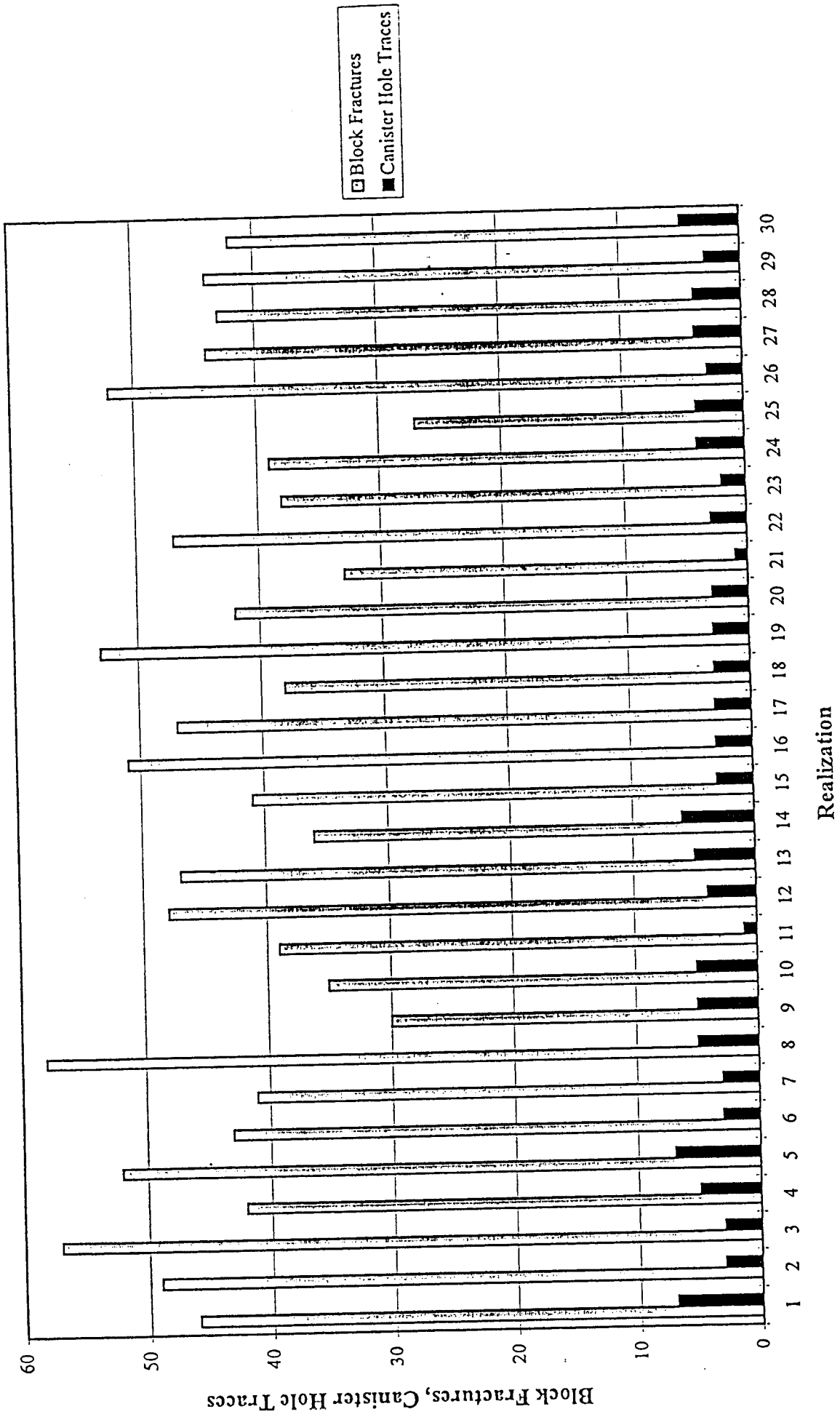

Figure 5-1 No. of Block Fractures No. of Canister Hole Traces for each realization.

Figure 5-1

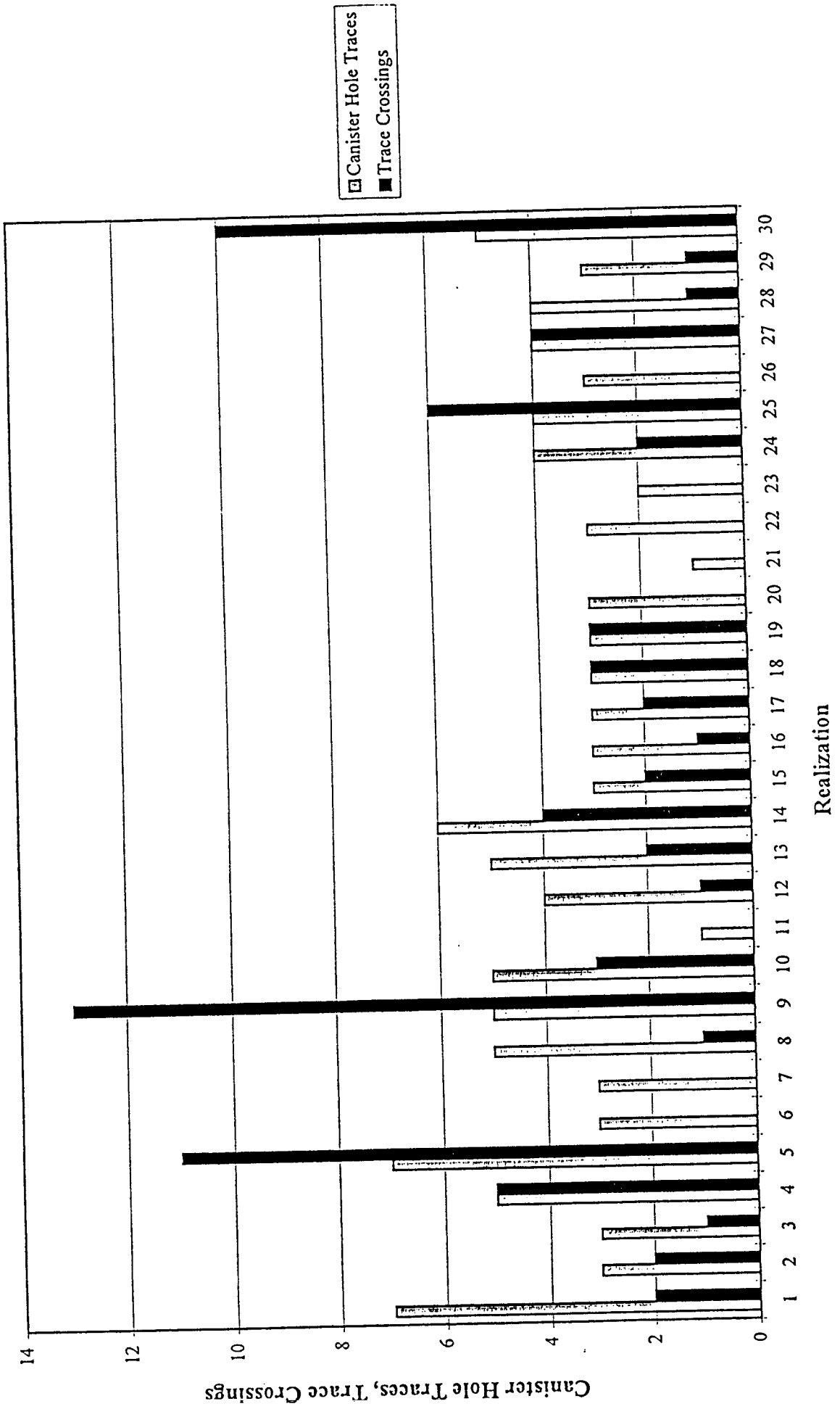

Figure 5-2

Figure 5-2 No. of Canister Hole Traces Crossings for each realization.

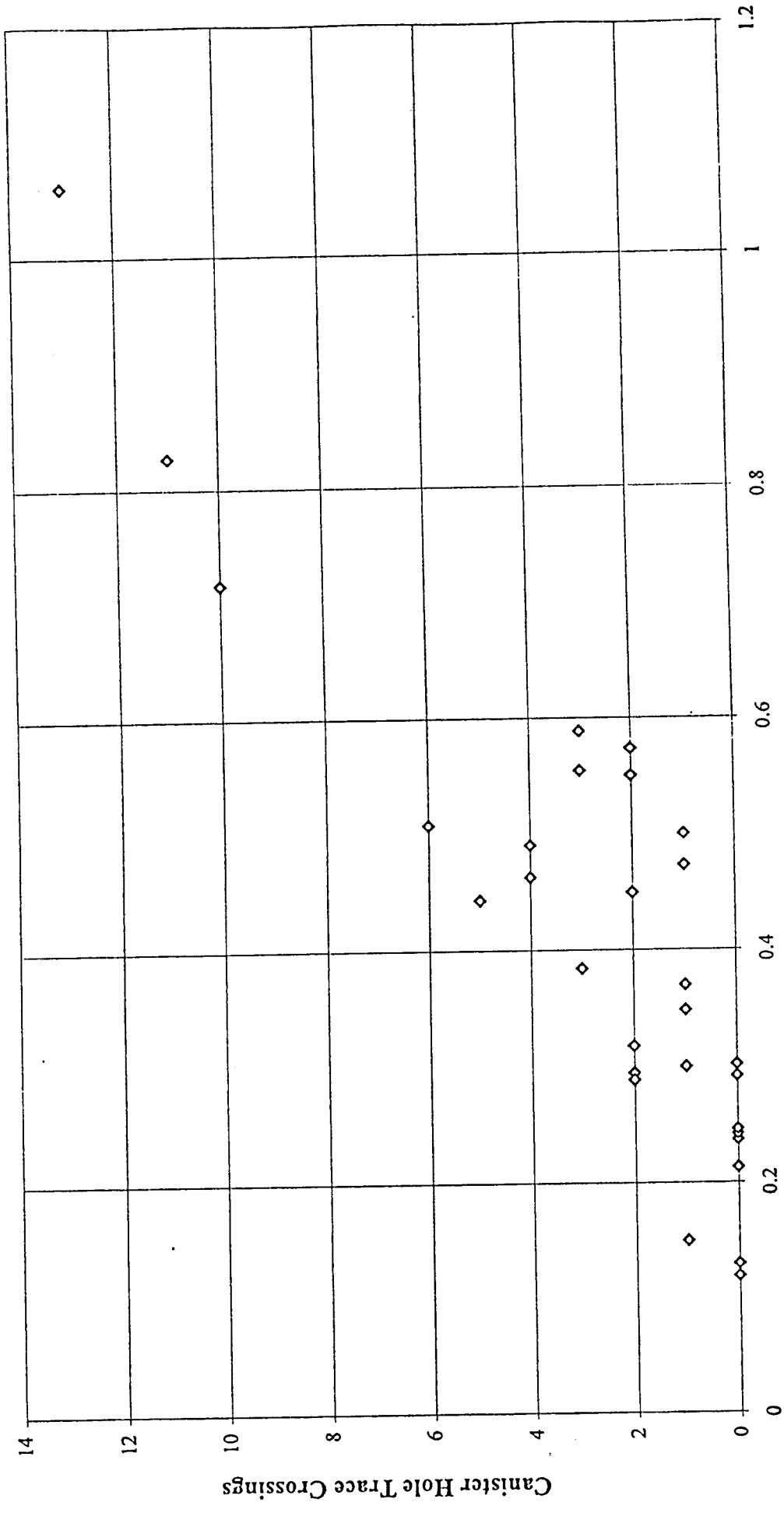

Figure 5-3 Canister Hole Traces vs. P_{21}-CAN.

Figure 5-3

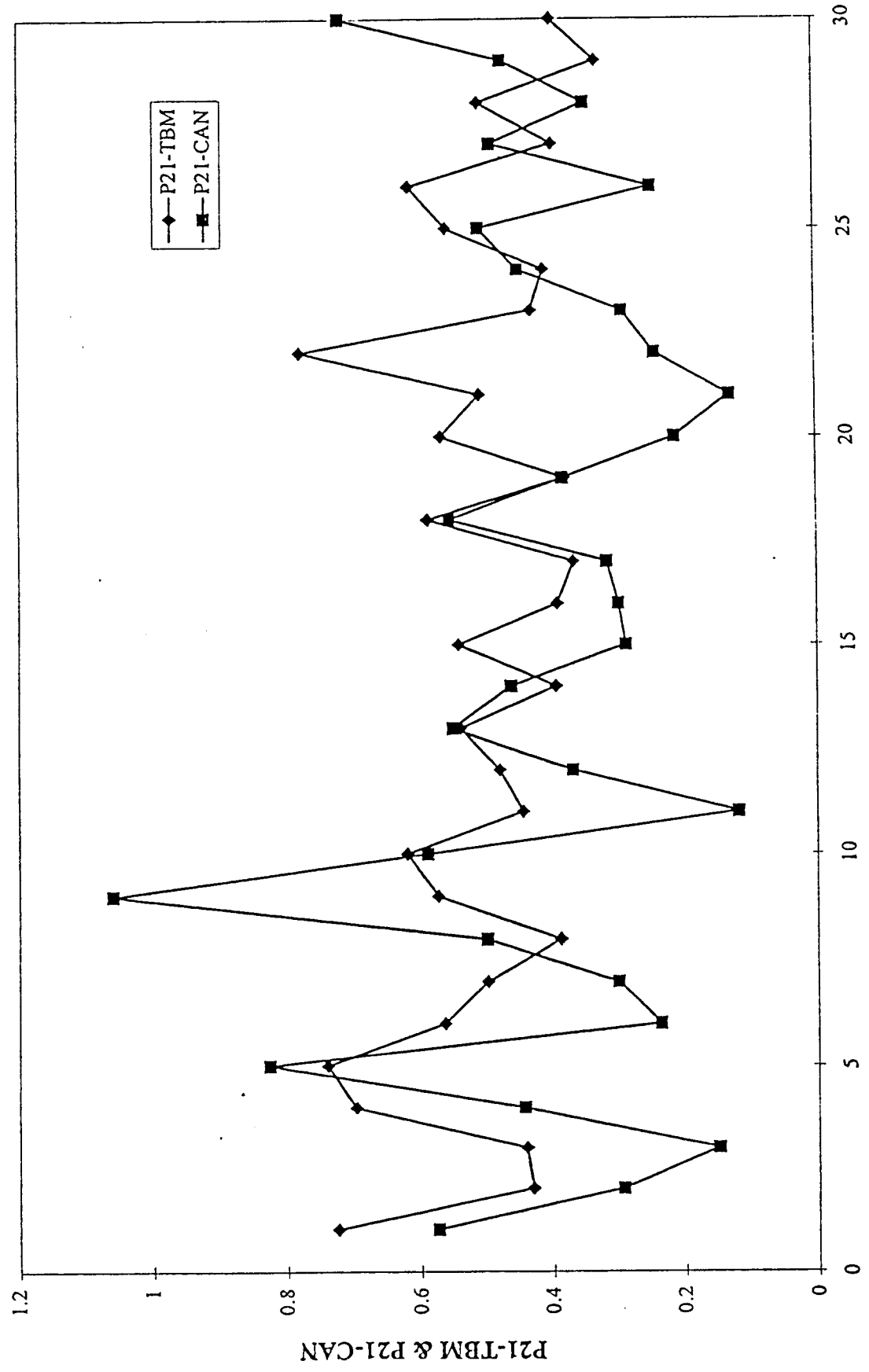

Figure 5-4 P_{21}-TBM and P21-CAN for each realization.

Figure 5-4

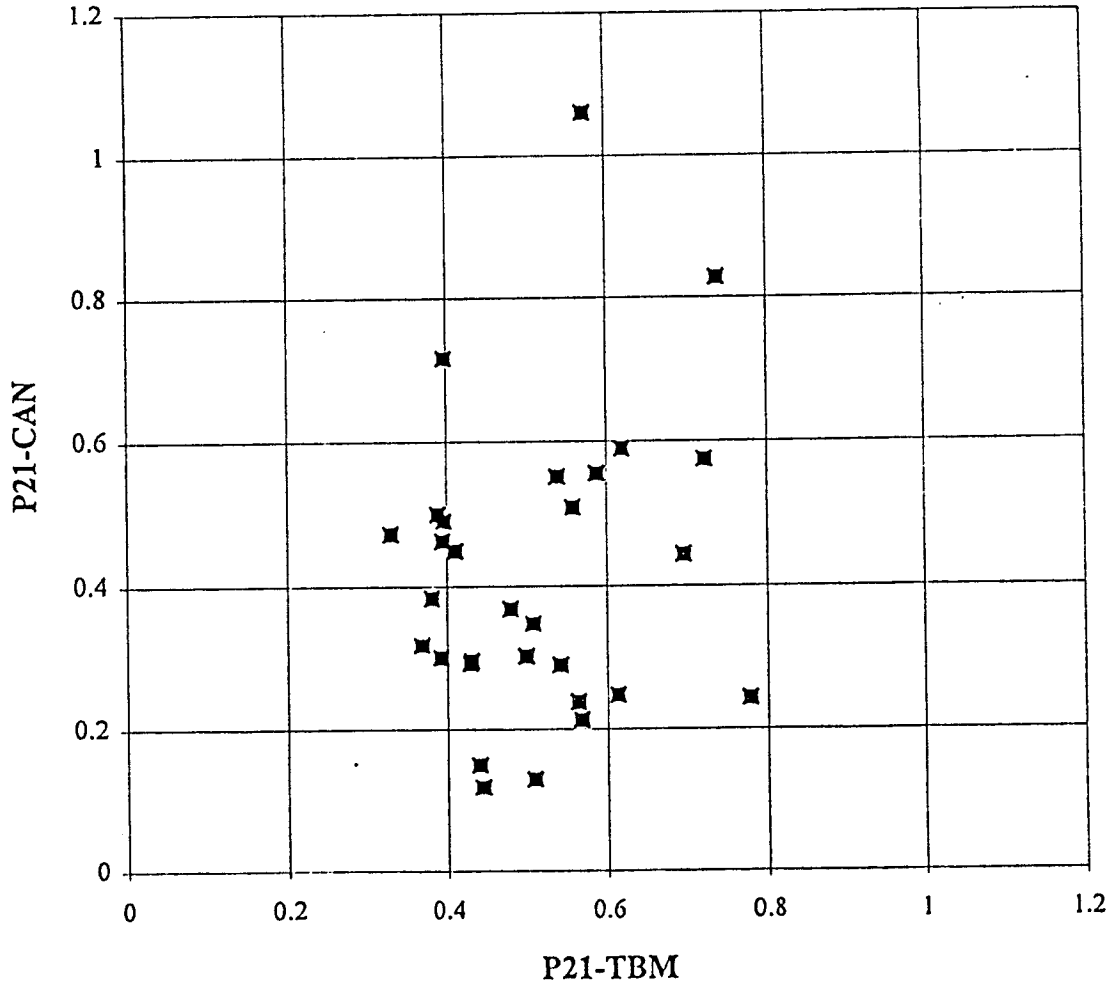

Figure 5-5 P_{21}-CAN vs. P_{21}-TBM.

Figure 5-5

REFERENCES

Dershowitz, W. & H. Herda(1992) Interpretation of fracture spacing and intensity, In Tillerson & Wawersik (Eds.): Roch mechanics, Balkema, RotherdamMassachusetts Institute of Technology, Cambridge, MA.

Dershowitz,W., A Thomas & Busse (1996) Discrete fracture analysis in support of the Äspö Tracer Retention Understanding Experiment (TRUE-1), Swedish Nuclear Fuel and Waste Management Co., ICR 96-05

Hermanson, J. (1995) Structural geology of water bearing fractures, Swedish Nuclear Fuel and Waste Management Co., SKB PR 25-95-23, Stockholm.

La Pointe, P., P. Wallman & W. Dershowitz (1993) Stochastic estimation of fracture size through simulated sampling, J. Rock. Mech. Min. Sci. & Geomech. Abstr. , 30(7), 1611-1617.

La Pointe, P., P. Wallman & S. Follin, (1995) Estimation of effective block conductivities based on discrete network analyses using data from the Äspö site, Swedish Nuclear Fuel and Waste Management Co., SKB TR 95-15, Stockholm.

Munier, R. (1993) Segmentation, fragmentation and jostling of the Baltic shield with time, Almquist & Wiksell International, Stockholm, 96 pp.

Munier, R. (1995) Studies of geological structures at Äspö - Comprehensive summary of results, Swedish Nuclear Fuel and Waste Management Co., SKB PR 25-95-21, Stockholm.

Stanfors, R. (1996) Personal communications.

APPENDICES

Appendix A:

1. Translation of Fractures from 2-D to 3-D
2. Translation of Mapping Cells (2-D) to tunnel panels (3-D)
3. Translation of Fracture Zones from 2-D to 3-D

Document written by Mr. Per EkströmVBB Anläggning AB, 1996-06-10.

Appendix B: Transformations of the Log-Normal Distribution

Appendix C: Excerpt of Canister Trace Maps

APPENDIX A

A1. TRANSLATION OF FRACTURES FROM 2-D TO 3-D

The 2D-fractures has been translated to 3D-fractures in the following steps:

1. Get geometrical data for the tunnel.
2. Translate curves describing fractures from 2D to 3D.
3. Merge all curves that belongs to the same fracture (e.g. curves connected so the same row in the database) into one curve.
4. Measure centriods and points along the 3D-fractures and load the data into *frac3d.dbf*.

The different steps are described in detail in the following chapters.

A1.1 Get geometrical data for the tunnel

The theoretical centerline (3D) is collected from different drawings and stored in a 3D-dgnfile. The contour line for the left and right wall is collected from different 2D-dgnfiles (tunnel?.dgn).

Input: 3D-centerline:Drawings numbered -063E, -064E, -067C, -901F, -902C.
Tunnel contours: tunnel1.dgn, tunnel2.dgn, tunnel4.dgn, tunnel5.dgn, tunnel6.dgn, tunneltb.dgn.

Output: *master.dgn*

Correlation between tunnel width and tunnel section is programmed into the translation routines.

Input: Section drawings numbered 1-081D, M16:19/0032-903B.

A1.2 Translate fractures from 2-D to 3-D

Curves describing fractures has been translated from 2D to 3D in the following steps:

1. Locate the 2D-curve describing the fracture.
2. Calculate points at every 0.1 m along the 2D-curve.
3. Translate all of these points to 3D in the following manner.
   I. Calculate the perpendicular point on the centerline (2D)
   II. Measure the perpendicular distance from the point to the centerline (2D).
   III. Project the point to the 3D centerline
   IV. Check the tunnel width by measuring the distance (perpendicular to the centerline) between the tunnel walls and get the theoretical tunnel section from the width - section correlation.
   V. Project the point along the theoretical tunnel section at the distance calculated in b).

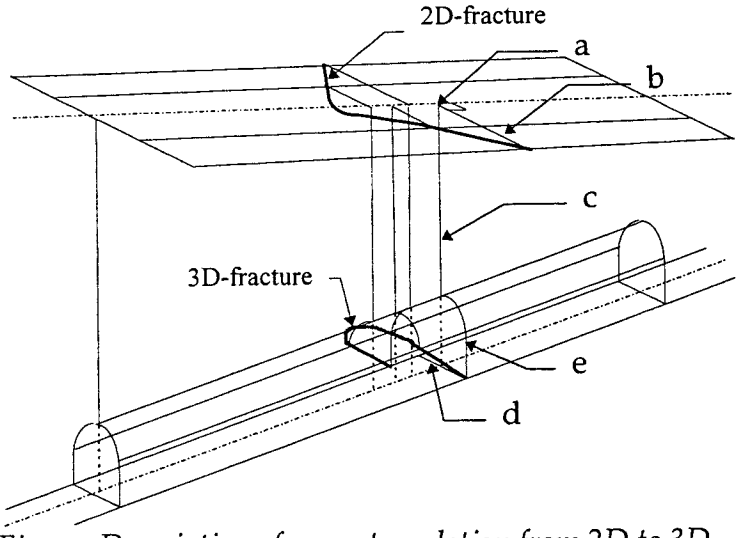

Figure. Description of curve translation from 2D to 3D.

Input: 2D-fracture files (*tkart1.dgn, tkart2.dgn, tkart3.dgn, tkart4.dgn, tkart5.dgn, tkarttbm.dgn, tkartz.dgn, master.dgn)*

Output: 3D-fracture files (*tk1fr3d.dgn, tk2fr3d.dgn, tk3fr3d.dgn, tk3fr3d.dgn, tk4fr3d.dgn, tk5fr3d.dgn, ttmbfr3b.dgn, tkzfr3d.dgn*)

A1.3 Create complex element

In many cases there is more than one curve in the design file that belongs to the same fracture (e.g. many curves points to the same row in the database). All curves connected to the same row in DB are merged into one element. (complex string), to enable measuring of total element length

There are some type fractures were we have problems merging the curves into one element.
These fractures are copied into a separate design file (*cmplx.dgn*) and if possible edited so that they can be merged into one element.

There are mainly two types of fractures were we have had problems merging them into one element.

1. Complex fractures

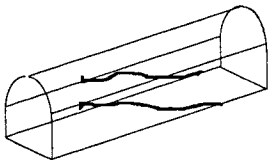

Only one side of the fracture will be measured and stored in the database.

2. Combinations with slicken slide

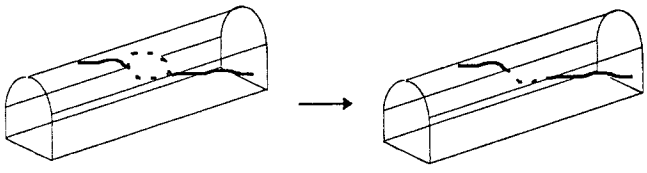

The part of the slicken slide that disable merging into one element is deleted manually, then the element is merged into one element.

Input: 3D-fracure files (*tk1fr3d.dgn, tk2fr3d.dgn, tk3fr3d.dgn, tk3fr3d.dgn, tk4fr3d.dgn, tk5fr3d.dgn, ttmbfr3b.dgn, tkzfr3d.dgn*)

Output: 3D-fracture files (*tk1fr3d.dgn, tk2fr3d.dgn, tk3fr3d.dgn, tk3fr3d.dgn, tk4fr3d.dgn, tk5fr3d.dgn, ttmbfr3b.dgn, tkzfr3d.dgn*) with all complex fractures marked red (co=3).
Fracture file with edited "problem" elements (*cmplx?.dgn*)

A1.4 Load fracture data in database

For every fracture we measure curve length, maximum length between two vertices on the curve, centriod and ten points along the curve and store the data in a dBase file (*frac3d.dbf*).

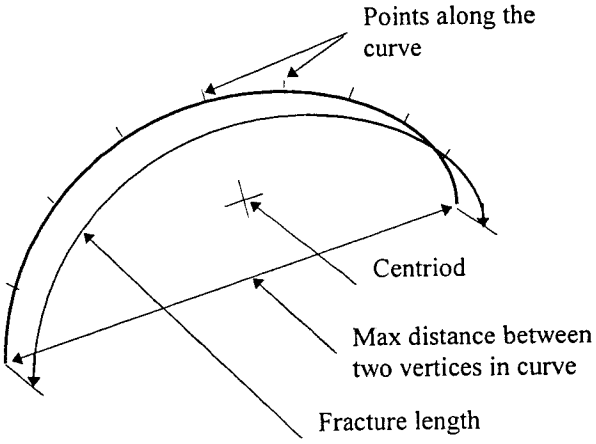

Figure. Description of measurement values from fracture

Description of *frac3d.dbf*:

Column name	Type	Description
ID	char(8)	Unique fracture-ID (ex A093603) 1: TUNNEL,2-5:SECTION(without decimal),6-7:FRAC_ID
TUNNEL	char(2)	Tunnel-ID
SECTION	numeric(6,1)	Section-ID
FRAC_ID	char(2)	Fracture-ID
FTC	char(1)	Fracture class: '0'=Normal, '1'=Complex, '2'=Slicken slide
XC	numeric(9,3)	Centroid X
YC	numeric(9,3)	Centroid Y
ZC	numeric(9,3)	Centroid Z
L_TOT	numeric(4,1)	Total fracture length
L_MAX	numeric(4,1)	Maximum distance between two points on fracture
X1	numeric(9,3)	Starting X on fracture
Y1	numeric(9,3)	Starting Y on fracture
Z1	numeric(9,3)	Starting Z on fracture
X2	numeric(9,3)	X for n/9-point on fracture
Y2	numeric(9,3)	Y for n/9-point on fracture
Z2	numeric(9,3)	Z for n/9-point on fracture
------	-----	----
X10	numeric(9,3)	Ending X on fracture
Y10	numeric(9,3)	Ending Y on fracture
Z10	numeric(9,3)	Ending Z on fracture
MSLINK	numeric(10,0)	Link to MicroStation

The columns TUNNEL, SECTION, FRAC_ID, MSLINK in *frac3d.dbf* are identical with the columns with the same name in *fracture.dbf*. The entity number for fracure elements is 10.

FTC
If some part of the fracture is "slicken slide", the fracture will be classified with FTC='2'. If a fracture is both "slicken slide" and "complex", the fracture will be classified as "complex", e.g. FTC='1'.

Input: 3D-fracture files. Input: 3D-fracure files (*tk1fr3d.dgn, tk2fr3d.dgn, tk3fr3d.dgn, tk3fr3d.dgn, tk4fr3d.dgn, tk5fr3d.dgn, ttmbfr3b.dgn, tkzfr3d.dgn, cmplx?.dgn*)

Fracture dbf-file (*fracture.dbf*)

Output: 3D-fracture files (*tk1fr3d.dgn, tk2fr3d.dgn, tk3fr3d.dgn, tk3fr3d.dgn, tk4fr3d.dgn, tk5fr3d.dgn, ttmbfr3b.dgn, tkzfr3d.dgn*) with all elements pointing to a non existing row in the database marked green (co=2).

dBase file with 3d-fracture data (*frac3d.dbf*).

A2. TRANSLATION OF MAPPING CELLS (2-D) TO TUNNEL PANELS (3-D)

The 2D-mapping cells has been translated to 3D-panels in the following steps:

1. Get geometrical data for the tunnel (see 1.1).
2. Translate mapping cells (2D) to tunnel panels (3D) (see 2.1).
3. Load panel data into *panel.dbf* (see 2.2).

A2.1 Translate maping cells to tunnel panels

Mapping cells has been translated to tunnel panels in the following steps:

1. Locate the mapping cell.
2. Calculate intersection points between the 2D-centerline and the mapping cell and the tunnel walls and the maping cell (6 nodes) (a).
3. Check the tunnel width by measuring the distance (perpendicular to the centerline) between the tunnel walls and get the theoretical tunnel section from the width - section correlation.
4. Get the z-value for the calculated intersections from the 3D-centerline (b).
5. Create panels with four nodes. The fourth node is forced into the the same plane as the three first nodes. The floor nodes in the wall panels are projected in the z-axis from the top wall nodes.

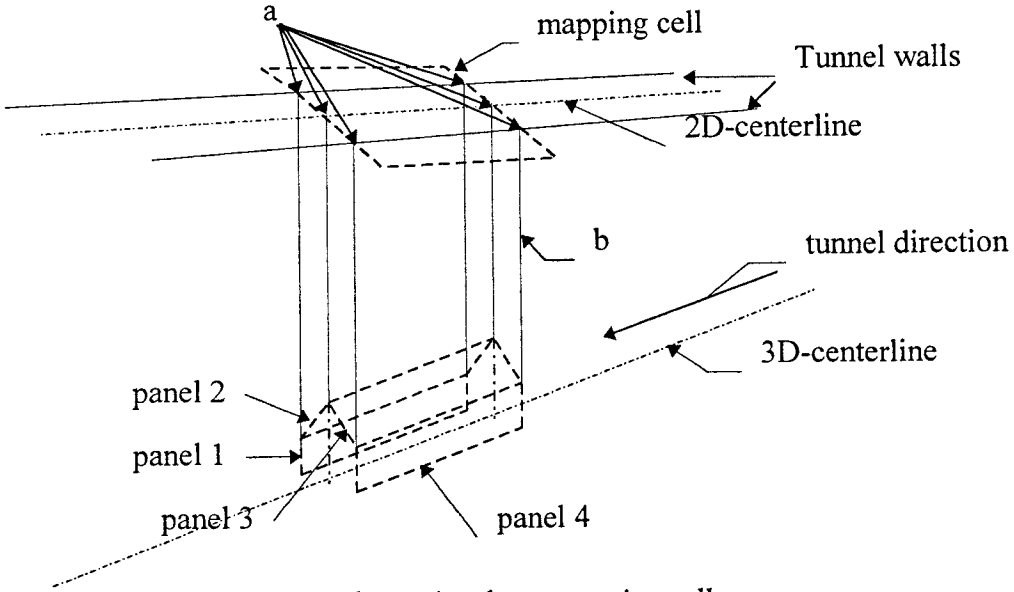

Figure. Description of panel creation from mapping cells.

In the TBM-tunnel the mapping cell is translated into six panels instead of four.

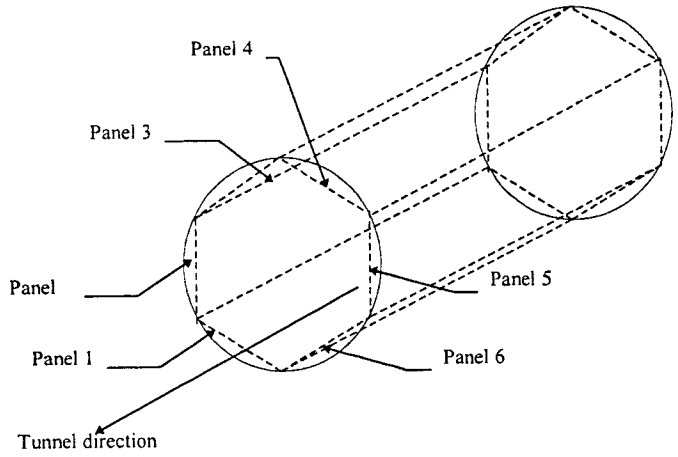

Figure. Description of panels in TBM-tunnel.

Input: 2D-mapcells (*tkart1.dgn, tkart2.dgn, tkart3.dgn, tkart4.dgn, tkart5.dgn, tkarttbm.dgn, master.dgn)*

Output: 3D-panel file (*panel.dgn*)

A2.2 Load panel data in database

Panel data is stored in a dBase file (*panel.dbf*).

Description of *panel.dbf* :

Column name	Type	Description
TUNNEL	char(2)	Tunnel-ID
SECTION	numeric(6,1)	Section-ID
SECT_LEN	numeric(4,1)	Section length (m)
PANEL	numeric(1,0)	1=right wall, 2=right roof, 3=left roof, 4=left wall
X1	numeric(9,3)	1:st node X
Y1	numeric(9,3)	1:st node Y
Z1	numeric(9,3)	1:st node Z
X2	numeric(9,3)	2:nd node X
Y2	numeric(9,3)	2:nd node Y
Z2	numeric(9,3)	2:nd node Z
X3	numeric(9,3)	3:rd node X
Y3	numeric(9,3)	3:rd node Y
Z3	numeric(9,3)	3:rd node Z
X4	numeric(9,3)	4:th node X
Y4	numeric(9,3)	4:th node Y
Z4	numeric(9,3)	4:th node Z
MSLINK	numeric(10,0)	Link to MicroStation

The columns TUNNEL and SECTION in *panel.dbf* are identical with the columns with the same name in *mapcell.dbf*. The entity number for panels is 11.

A3. TRANSLATION OF FRACTURE ZONES FROM 2D TO 3D

The 2D-curves describing the fracture zones are translated to 3D in the same manner as fractures (se 1.1). After the curves are tranlated to 3D we manually create a closed polygon. The elements that connect the translated curves are created manually and follow the floor nodes of tunnel panels.

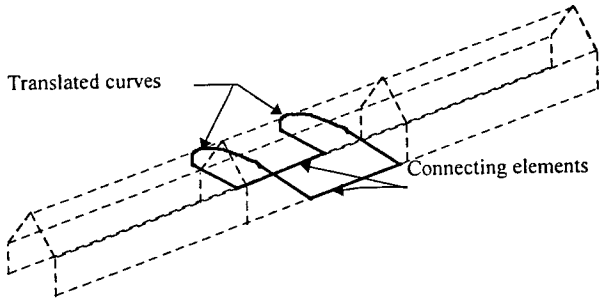

Figure. Description offracture zones.

Input: 2D-fracture zones (*tkart1.dgn, tkart2.dgn, tkart3.dgn, tkart4.dgn, tkart5.dgn, tkarttbm.dgn, tkartz.dgn, master.dgn)*

Output: 3D-fracture zones (*frzon3d.dgn*)

A3.1 Load fracture zone data in database

For the fracture zone we calculate coordinates and store in a dbf-file. The distance between the calculated coordinates is 1 meter (*frac3d.dbf*). The information for fracture zones are stored in two dbf-files, *frzon3d.dbf* and *frzonpts.dbf*. The general information is stored in *frzon3d.dbf* and the node data is stored in *frzonpts.dbf*. The two tables are jointed thru the column *ID*.

There is only one row in *frzon3d.dbf* for every fracture zone. In *fraczon1.dbf* there is often many rows connected to the same fracture zone, one for every included section. In *frzon3d.dbf* the lowest section is used.

Description of *frzon3d.dbf*:

Column name	Type	Description
ID	char(8)	Unique fracture-ID (ex A093603) 1: TUNNEL,2-5:SECTION(without decimal),6-7:ZONE_ID
TUNNEL	char(2)	Tunnel-ID
SECTION	numeric(6,1)	Section-ID
ZONE_ID	char(2)	Zone-ID,
NUMPTS	numeric(5,0)	Number of nodes for zone in *frzonpts.dbf*
MSLINK	numeric(10,0)	Link to MicroStation

Description of *frzonpts.dbf*:

Column name	Type	Description
ID	char(8)	Unique link-ID to *frzon3d.dbf*
PNUM	numeric(5,0)	Node number
X	numeric(9,3)	X
Y	numeric(9,3)	Y
Z	numeric(9,3)	Z

The columns TUNNEL, SECTION, ZONE_ID, MSLINK in *frzon3d.dbf* are identical with the columns with the same name in *fraczon1.dbf*. The entity number for panels is 12.

Per Ekström
VBB Anläggning AB
CAD-teknik

APPENDIX B

B1. TRANSFORMATIONS OF THE LOG-NORMAL DISTRIBUTION

The log-normal distribution is given by the function

$$f(x) = \frac{1}{x\ln(10)y_\alpha\sqrt{2\pi}}\exp\{-\frac{1}{2}(\frac{\log x - \bar{y}}{y_\alpha})^2\}$$

Where $\bar{y}$ and y_α is mean and standard deviation in $\log_{10}$ space. In FracMan the logarithmic distribution is defined by the mean and standard deviation in real space (arithmetic). This is to provide a mean in units of meters which is a comprehensible measure of fracture size. This is despite the fact that the standard deviation in real space is more complex to understand. There exists simple conversion formulas between $\log_{10}$ space and real space. Given the $\bar{y}$ and y_α the arithmetic mean $\bar{x}$, and standard deviation x_α is

$$\bar{x} = e^{(c\bar{y}+1/2(cy_\alpha)^2}$$

and

$$x_\alpha = \bar{x}\sqrt{e^{(cy_\alpha)^2} - 1}$$

and vice versa, i.e. given $\bar{x}$ and x_α

$$\bar{y} = \frac{1}{c}(\ln(\bar{x}) - \frac{(cy_\alpha)^2}{2})$$

$$y_\alpha = \frac{1}{c}\sqrt{\ln(1+(\frac{x_\alpha}{\bar{x}})^2)}$$

where c is the natural log of 10 (≈ 2.302).

APPENDIX C

EXCERPT OF CANISTER TRACE MAPS

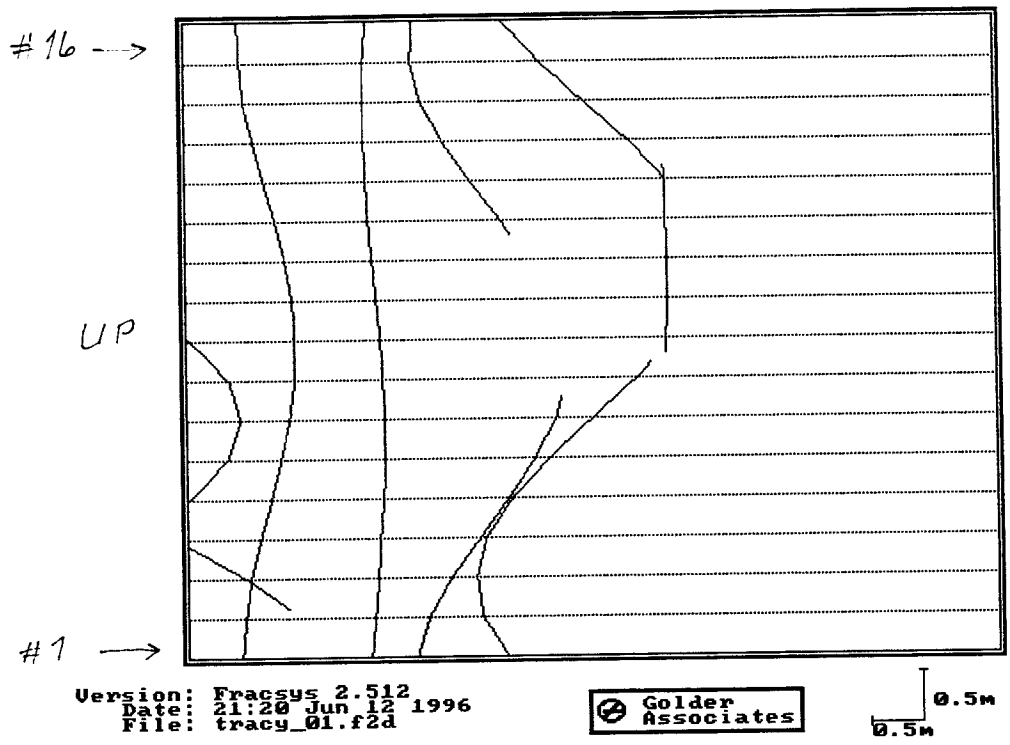

Tracy_01.sts created by FracWorks 2.512 13:40 Apr 26 1996
Macro: AUTOWORK.MAC File: can_01.dcm

==========

# of fracs in system : 46 P32: .480 m^2/m^3

# of fracs connected to traceplanes: 7 # of traces: 7

Group # of Planes Planes:
1 16: 1 2 3 4 5 6 7 8 9 10 11 12 13 14 15 16

Group	# of Fracs	# of [Xs, Ts, Ends]			Trace (m)
1	7	2	0	7	4.17

of [Xs+Ts]/sq.m = .3928E-01
of Frac / sq.m = .1375E+00
Termination prob. = .0000E+00
Termination pct = .0000E+00
Intensity (m/sq.m) = .5739E+00

Frac Stats Mean +- Std. Dev. (Min, Max)

Trace Length [m] 4.17E+00 +- 2.38E+00 (1.17E+00, 6.48E+00)
Trans. [m^2/s] 1.00E-06 +- 3.51E-11 (1.00E-06, 1.00E-06)
Cond. [m^3/s] 4.17E-06 +- 2.38E-06 (1.17E-06, 6.48E-06)

*** Total conductance : 2.922E-05 ***

REALIZATION 2

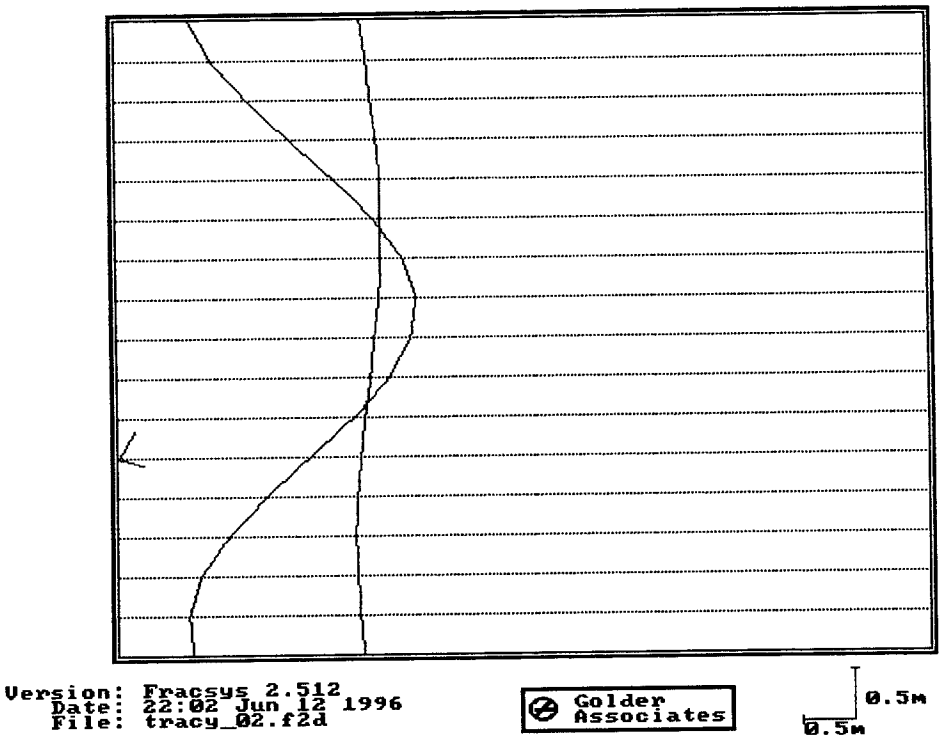

Tracy_02.sts created by FracWorks 2.512 13:41 Apr 26 1996
Macro: AUTOWORK.MAC File: can_02.dcm

==========

# of fracs in system : 49 P32: .472 m^2/m^3

# of fracs connected to traceplanes: 3 # of traces: 3

Group # of Planes Planes:
1 16: 1 2 3 4 5 6 7 8 9 10 11 12 13 14 15 16

Group # of Fracs # of [Xs, Ts, Ends] Trace (m)
1 3 2 0 2 5.00

of [Xs+Ts]/sq.m = .3928E-01
of Frac / sq.m = .5892E-01
Termination prob. = .0000E+00
Termination pct = .0000E+00
Intensity (m/sq.m) = .2943E+00

Frac Stats Mean +- Std. Dev. (Min, Max)

Trace Length [m] 5.00E+00 +- 3.91E+00 (5.81E-01, 8.01E+00)
Trans. [m^2/s] 1.00E-06 +- 3.98E-11 (1.00E-06, 1.00E-06)
Cond. [m^3/s] 5.00E-06 +- 3.91E-06 (5.81E-07, 8.01E-06)

*** Total conductance : 1.499E-05 ***

REALIZATION 3

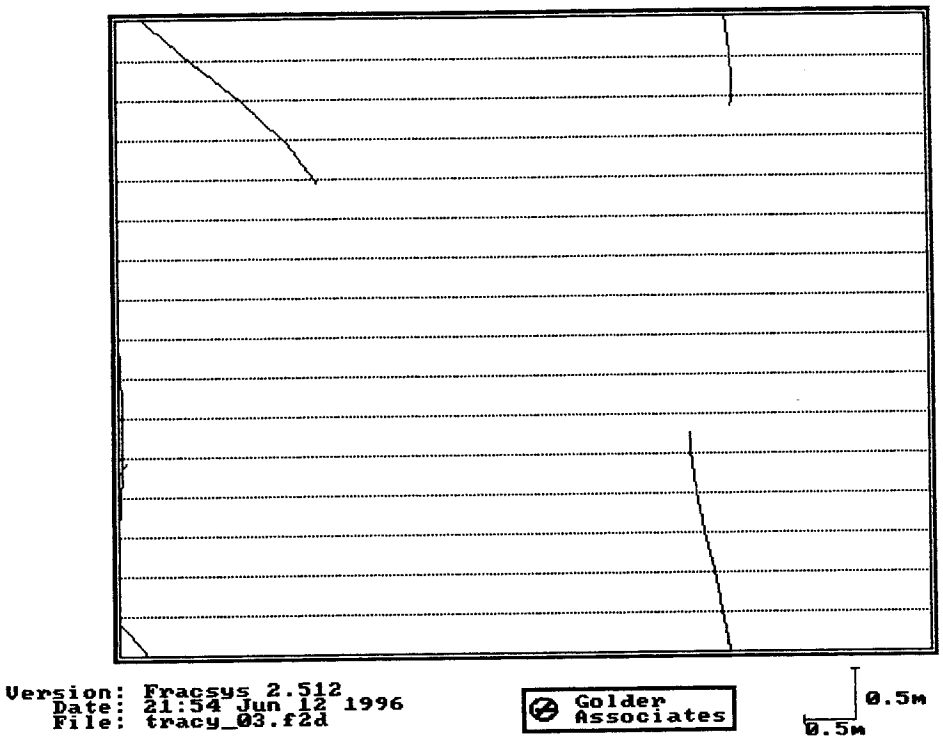

Tracy_03.sts created by FracWorks 2.512 13:41 Apr 26 1996
Macro: AUTOWORK.MAC File: can_03.dcm

==========

# of fracs in system : 57 P32: .482 m^2/m^3

# of fracs connected to traceplanes: 3 # of traces: 3

Group # of Planes Planes:
1 16: 1 2 3 4 5 6 7 8 9 10 11 12 13 14 15 16

Group # of Fracs # of [Xs, Ts, Ends] Trace (m)
1 3 1 0 4 2.55

of [Xs+Ts]/sq.m = .1964E-01
of Frac / sq.m = .5892E-01
Termination prob. = .0000E+00
Termination pct = .0000E+00
Intensity (m/sq.m) = .1503E+00

Frac Stats Mean +- Std. Dev. (Min, Max)

Trace Length [m] 2.55E+00 +- 7.92E-01 (1.65E+00, 3.12E+00)
Trans. [m^2/s] 1.00E-06 +- 3.98E-11 (1.00E-06, 1.00E-06)
Cond. [m^3/s] 2.55E-06 +- 7.92E-07 (1.65E-06, 3.12E-06)

*** Total conductance : 7.652E-06 ***

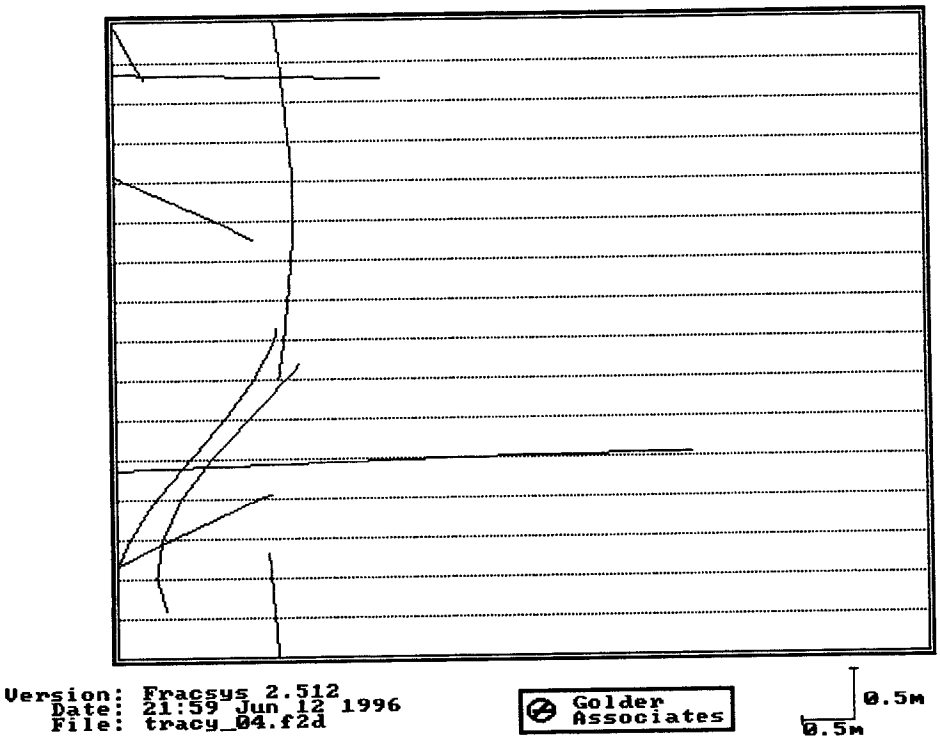

Tracy_04.sts created by FracWorks 2.512 13:41 Apr 26 1996
Macro: AUTOWORK.MAC File: can_04.dcm

# of fracs in system : 42 P32: .476 m^2/m^3

# of fracs connected to traceplanes: 5 # of traces: 5

Group # of Planes Planes:
1 16: 1 2 3 4 5 6 7 8 9 10 11 12 13 14 15 16

Group # of Fracs # of [Xs, Ts, Ends] Trace (m)
1 5 5 0 9 4.51

of [Xs+Ts]/sq.m = .9820E-01
of Frac / sq.m = .9820E-01
Termination prob. = .0000E+00
Termination pct = .0000E+00
Intensity (m/sq.m) = .4429E+00

Frac Stats Mean +- Std. Dev. (Min, Max)

Trace Length [m] 4.51E+00 +- 2.23E+00 (2.98E+00, 8.32E+00)
Trans. [m^2/s] 1.00E-06 +- 3.63E-11 (1.00E-06, 1.00E-06)
Cond. [m^3/s] 4.51E-06 +- 2.23E-06 (2.98E-06, 8.32E-06)

*** Total conductance : 2.255E-05 ***

REALIZATION 5

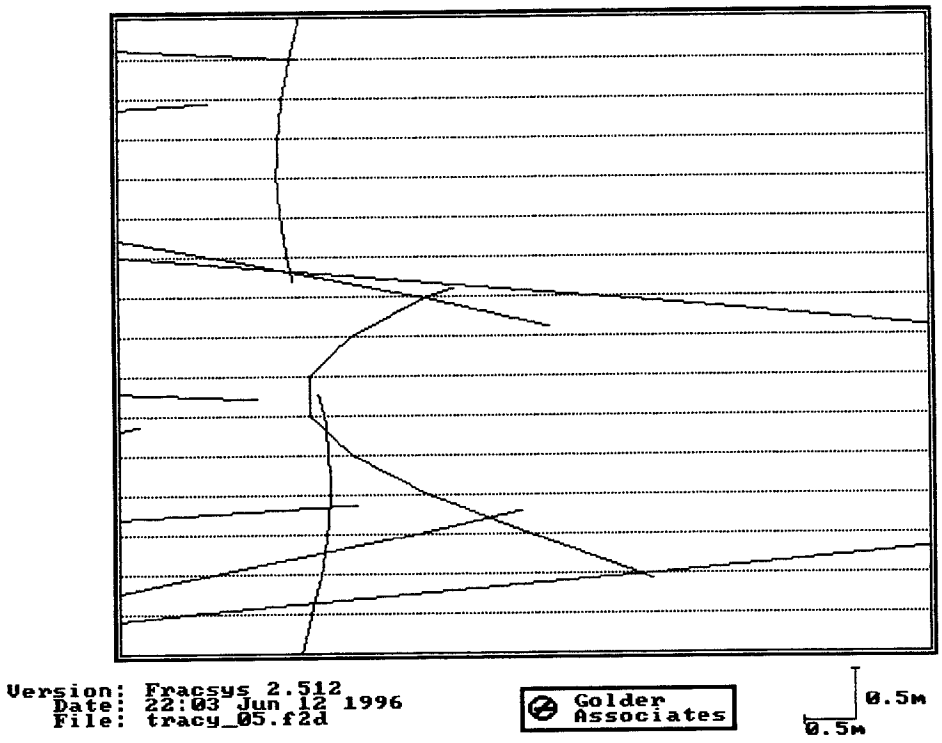

Tracy_05.sts created by FracWorks 2.512 13:41 Apr 26 1996
Macro: AUTOWORK.MAC File: can_05.dcm

# of fracs in system : 52 P32: .486 m^2/m^3

# of fracs connected to traceplanes: 7 # of traces: 7

Group # of Planes Planes:
1 16: 1 2 3 4 5 6 7 8 9 10 11 12 13 14 15 16

Group	# of Fracs	# of [Xs, Ts, Ends]			Trace (m)
1	7	11	0	10	6.02

of [Xs+Ts]/sq.m = .2160E+00
of Frac / sq.m = .1375E+00
Termination prob. = .0000E+00
Termination pct = .0000E+00
Intensity (m/sq.m) = .8272E+00

Frac Stats	Mean	+- Std. Dev.	(Min, Max)
Trace Length [m]	6.02E+00	+- 5.15E+00	(1.80E-01, 1.61E+01)
Trans. [m^2/s]	1.00E-06	+- 3.51E-11	(1.00E-06, 1.00E-06)
Cond. [m^3/s]	6.02E-06	+- 5.15E-06	(1.80E-07, 1.61E-05)

*** Total conductance : 4.212E-05 ***

REALIZATION 6

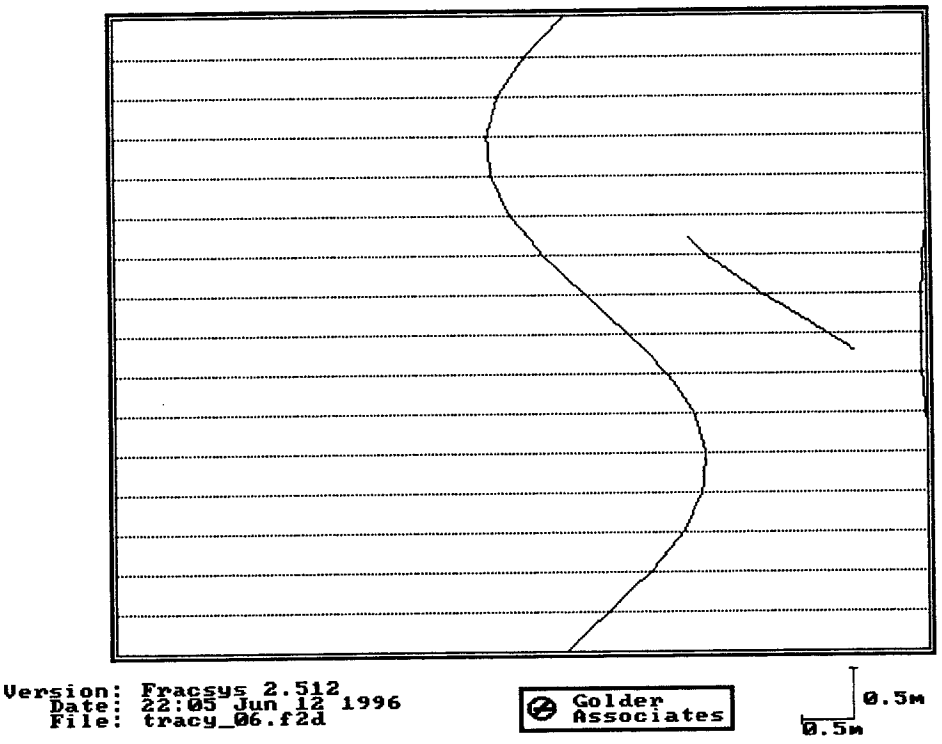

Tracy_06.sts created by FracWorks 2.512 13:41 Apr 26 1996
Macro: AUTOWORK.MAC File: can_06.dcm

# of fracs in system : 43 P32: .478 m^2/m^3

# of fracs connected to traceplanes: 3 # of traces: 3

Group # of Planes Planes:
1 16: 1 2 3 4 5 6 7 8 9 10 11 12 13 14 15 16

Group	# of Fracs	# of [Xs, Ts, Ends]			Trace (m)
1	3	0	0	2	4.02

of [Xs+Ts]/sq.m = .0000E+00
of Frac / sq.m = .5892E-01
Termination prob. = .0000E+00
Termination pct = .0000E+00
Intensity (m/sq.m) = .2371E+00

Frac Stats	Mean	+- Std. Dev.	(Min, Max)
Trace Length [m]	4.02E+00	+- 3.35E+00	(1.98E+00, 7.90E+00)
Trans. [m^2/s]	1.00E-06	+- 3.98E-11	(1.00E-06, 1.00E-06)
Cond. [m^3/s]	4.02E-06	+- 3.35E-06	(1.98E-06, 7.90E-06)

*** Total conductance : 1.207E-05 ***

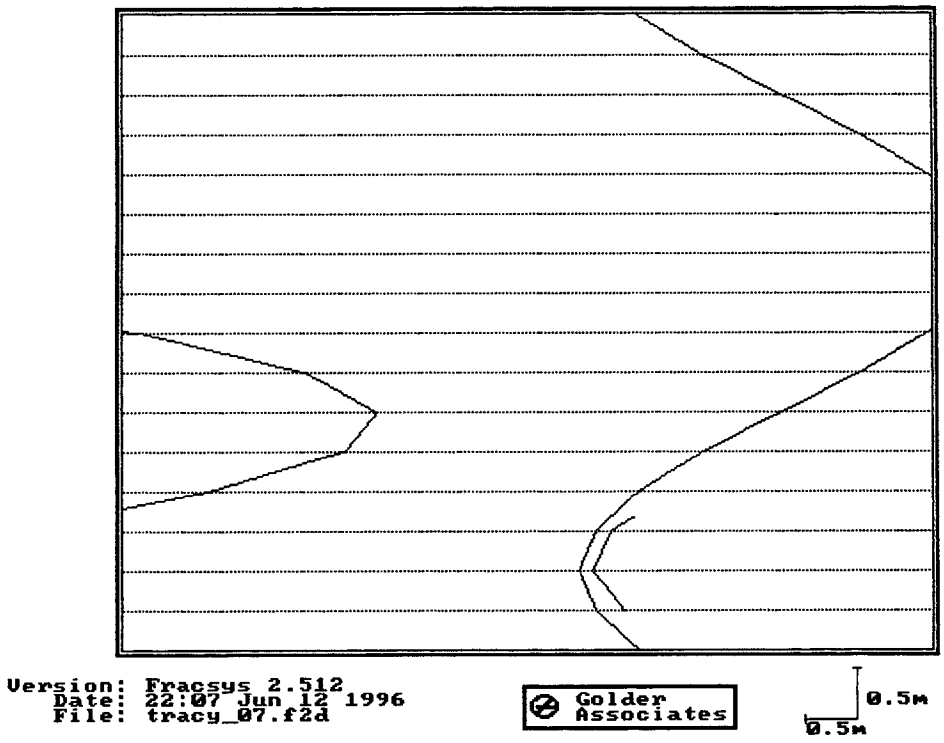

Tracy_07.sts created by FracWorks 2.512 13:41 Apr 26 1996
Macro: AUTOWORK.MAC File: can_07.dcm

# of fracs in system : 41 P32: .488 m^2/m^3

# of fracs connected to traceplanes: 3 # of traces: 3

Group # of Planes Planes:
1 16: 1 2 3 4 5 6 7 8 9 10 11 12 13 14 15 16

Group # of Fracs # of [Xs, Ts, Ends] Trace (m)
1 3 0 0 2 5.11

of [Xs+Ts]/sq.m = .0000E+00
of Frac / sq.m = .5892E-01
Termination prob. = .0000E+00
Termination pct = .0000E+00
Intensity (m/sq.m) = .3012E+00

Frac Stats Mean +- Std. Dev. (Min, Max)

Trace Length [m] 5.11E+00 +- 3.75E+00 (1.20E+00, 8.69E+00)
Trans. [m^2/s] 1.00E-06 +- 3.98E-11 (1.00E-06, 1.00E-06)
Cond. [m^3/s] 5.11E-06 +- 3.75E-06 (1.20E-06, 8.69E-06)

*** Total conductance : 1.534E-05 ***

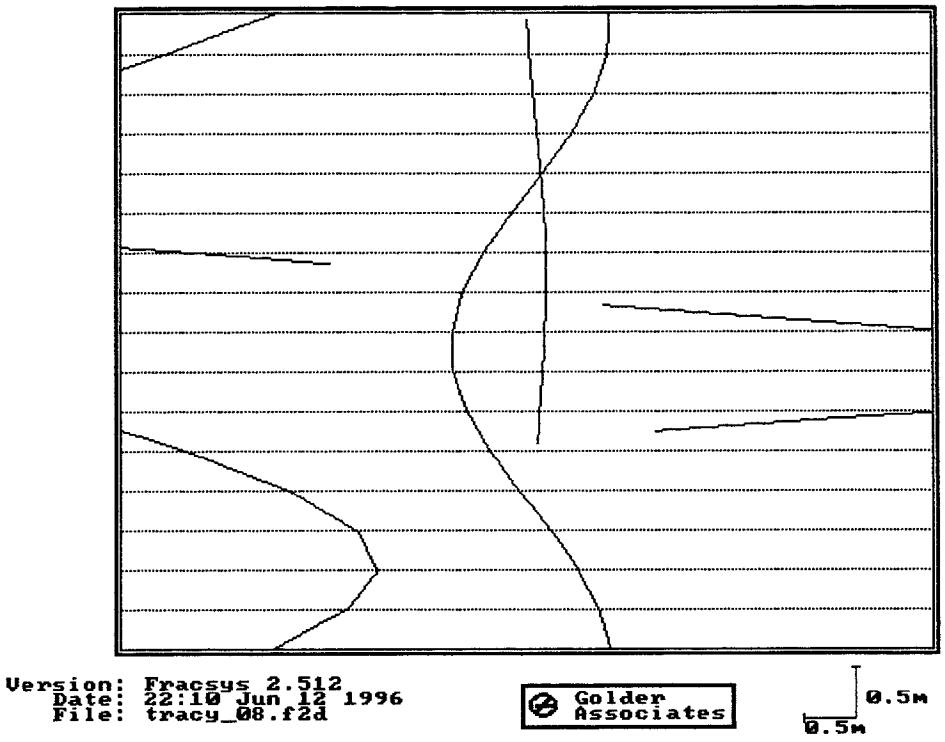

Tracy_08.sts created by FracWorks 2.512 13:42 Apr 26 1996
Macro: AUTOWORK.MAC File: can_08.dcm

==========

# of fracs in system : 58 P32: .469 m^2/m^3

# of fracs connected to traceplanes: 5 # of traces: 5

Group # of Planes Planes:
1 16: 1 2 3 4 5 6 7 8 9 10 11 12 13 14 15 16

Group # of Fracs # of [Xs, Ts, Ends] Trace (m)
1 5 1 0 5 5.09

of [Xs+Ts]/sq.m = .1964E-01
of Frac / sq.m = .9820E-01
Termination prob. = .0000E+00
Termination pct = .0000E+00
Intensity (m/sq.m) = .4994E+00

Frac Stats Mean +- Std. Dev. (Min, Max)

Trace Length [m] 5.09E+00 +- 2.00E+00 (2.06E+00, 7.23E+00)
Trans. [m^2/s] 1.00E-06 +- 3.63E-11 (1.00E-06, 1.00E-06)
Cond. [m^3/s] 5.09E-06 +- 2.00E-06 (2.06E-06, 7.23E-06)

*** Total conductance : 2.543E-05 ***

REALIZATION 9

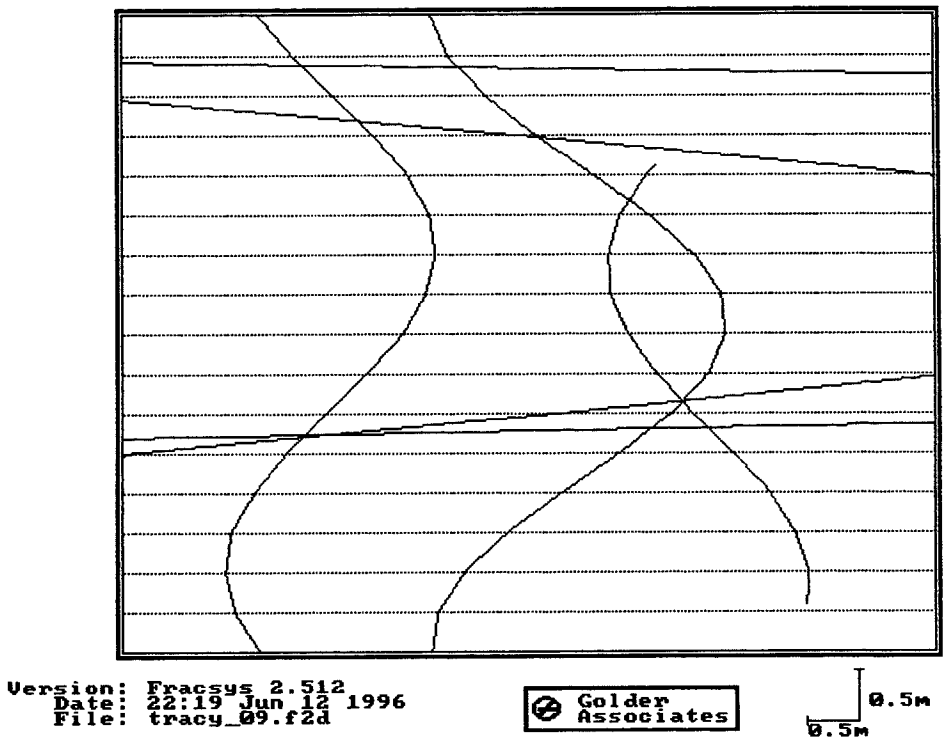

Tracy_09.sts created by FracWorks 2.512 13:42 Apr 26 1996
Macro: AUTOWORK.MAC File: can_9.dcm

==========

# of fracs in system : 30 P32: .471 m^2/m^3

# of fracs connected to traceplanes: 5 # of traces: 5

Group # of Planes Planes:
1 16: 1 2 3 4 5 6 7 8 9 10 11 12 13 14 15 16

Group # of Fracs # of [Xs, Ts, Ends] Trace (m)
1 5 13 0 2 10.8

of [Xs+Ts]/sq.m = .2553E+00
of Frac / sq.m = .9820E-01
Termination prob. = .0000E+00
Termination pct = .0000E+00
Intensity (m/sq.m) = .1060E+01

Frac Stats Mean +- Std. Dev. (Min, Max)

Trace Length [m] 1.08E+01 +- 4.97E+00 (5.19E+00, 1.61E+01)
Trans. [m^2/s] 1.00E-06 +- 3.63E-11 (1.00E-06, 1.00E-06)
Cond. [m^3/s] 1.08E-05 +- 4.97E-06 (5.19E-06, 1.61E-05)

*** Total conductance : 5.397E-05 ***

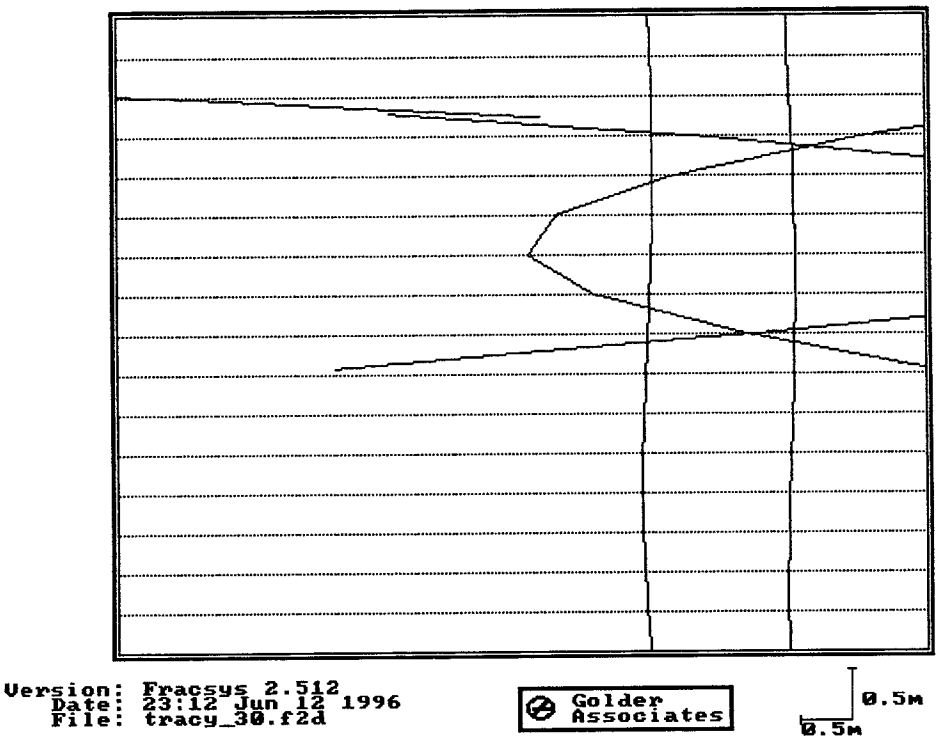

Tracy_30.sts created by FracWorks 2.512 13:45 Apr 26 1996
Macro: AUTOWORK.MAC File: can_30.dcm

==========

# of fracs in system : 42 P32: .479 m^2/m^3

# of fracs connected to traceplanes: 5 # of traces: 5

Group # of Planes Planes:
1 16: 1 2 3 4 5 6 7 8 9 10 11 12 13 14 15 16

Group # of Fracs # of [Xs, Ts, Ends] Trace (m)
1 5 10 0 3 7.30

of [Xs+Ts]/sq.m = .1964E+00
of Frac / sq.m = .9820E-01
Termination prob. = .0000E+00
Termination pct = .0000E+00
Intensity (m/sq.m) = .7170E+00

Frac Stats Mean +- Std. Dev. (Min, Max)

Trace Length [m] 7.30E+00 +- 2.63E+00 (4.20E+00, 1.12E+01)
Trans. [m^2/s] 1.00E-06 +- 3.63E-11 (1.00E-06, 1.00E-06)
Cond. [m^3/s] 7.30E-06 +- 2.63E-06 (4.20E-06, 1.12E-05)

*** Total conductance : 3.651E-05 ***